Supplementary Material

Investigating selective arsenate adsorption in presence of phosphate via ternary metal biopolymer composites with either Fe, Al, or Cu as active Lewis acid sites

Nam T. Bui[1], Bernd G.K. Steiger[1] and Lee D. Wilson[1]*

[1]Department of Chemistry, University of Saskatchewan, 110 Science Place, Saskatoon, S7N 5C9

*Corresponding author

Contents

Table of Tables **2**
Table of Figures **2**
Phosphate and Arsenate Determination **4**
FT-IR Spectroscopy **5**
Point-of-Zero (PZC) Determination **8**
Phosphate adsorption at pH 6.3 ..... **10**
Arsenate adsorption isotherms at pH 6.7 ..... **11**
Phosphate adsorption Isotherms at pH 8.5 ..... **14**
SEM-EDX Imaging **16**
Al-TMC 16
Cu-TMC 28
Fe-TMC 40

Table of Tables

Table S1: Results of the pH measurements to determine the PZC. 8
Table S2: Tabled ΔpH values and initial pH values used for PZC calculations. 9
Table S3: Isotherm parameters fit with Sips model for phosphate adsorption at pH6.3……..9
Table S4: Isotherm parameters fit with Sips model for arsenate adsorption at pH6.7……..11
Table S5: Isotherm parameters fit with Sips model for arsenate adsorption at pH8.5……..13

Table of Figures

Figure S1: FT-IR spectrum of Al-TMC. 5
Figure S2: FT-IR spectrum of Fe-TMC. 5
Figure S3: FT-IR spectrum of Cu-TMC. 6
Figure S4: FT-IR spectrum of Chitosan. 6
Figure S5: FT-IR spectrum of Sodium Alginate. 7
Figure S6: Change in pH vs initial pH plot. 8
Figure S7: Phosphate adsorption at pH 6.3 isotherm of Al-TMC. 10
Figure S8: Phosphate adsorption at pH 6.3 isotherm of Fe-TMC. 11
Figure S9:Phosphate adsorption at pH 6.3 isotherm of Cu-TMC. 11
Figure S10: Arsenate adsorption isotherm of Al-TMC. 12
Figure S11: Arsenate adsorption isotherm of Fe-TMC..... 13
Figure S12: Arsenate adsorption isotherm of Al-TMC. 13
Figure S13: Phosphate adsorption at pH 8.5 isotherm of Al-TMC. 14
Figure S14: Phosphate adsorption at pH 8.5 isotherm of Fe-TMC. 15
Figure S15: Phosphate adsorption at pH 8.5 isotherm of Cu-TMC. 15
Figure S16: SEM-EDX mapping of Al-TMC (spot 1). 16
Figure S17: Surface morphology and elemental composition of Al-TMC (spot 1). 17
Figure S18: SEM-EDX mapping of Al-TMC (spot 2). 18
Figure S19: Surface morphology and elemental composition of Al-TMC (spot 2). 19
Figure S20: SEM-EDX mapping of Al-TMC (spot 3). 20
Figure S21: Surface morphology and elemental composition of Al-TMC (spot 3). 21
Figure S22: SEM-EDX mapping of Al-TMC (spot 4). 22
Figure S23: Surface morphology and elemental composition of Al-TMC (spot 4). 23
Figure S24: SEM-EDX mapping of Al-TMC (spot 5). 24
Figure S25: Surface morphology and elemental composition of Al-TMC (spot 5). 25
Figure S26: SEM-EDX mapping of Al-TMC (spot 6). 26
Figure S27: Surface morphology and elemental composition of Al-TMC (spot 6). 27
Figure S28: SEM-EDX mapping of Cu-TMC (spot 2). 28
Figure S29: Surface morphology and elemental composition of Cu-TMC (spot 2). 29
Figure S30: SEM-EDX mapping of Cu-TMC (spot 3). 30
Figure S31: Surface morphology and elemental composition of Cu-TMC (spot 3). 31
Figure S32: SEM-EDX mapping of Cu-TMC (spot 4). 32
Figure S33: Surface morphology and elemental composition of Cu-TMC (spot 4). 33
Figure S34: SEM-EDX mapping of Cu-TMC (spot 5). 34
Figure S35: Surface morphology and elemental composition of Cu-TMC (spot 5). 35

Figure S36: SEM-EDX mapping of Cu-TMC (spot 6). 36
Figure S37: Surface morphology and elemental composition of Cu-TMC (spot 6). 37
Figure S38: SEM-EDX mapping of Cu-TMC (spot 7). 38
Figure S39: Surface morphology and elemental composition of Cu-TMC (spot 7). 39
Figure S40: SEM-EDX mapping of Fe-TMC (spot 1). 40
Figure S41:Surface morphology and elemental composition of Fe-TMC (spot 1). 41
Figure S42: SEM-EDX mapping of Fe-TMC (spot 2). 42
Figure S43: Surface morphology and elemental composition of Fe-TMC (spot 2). 43
Figure S44: SEM-EDX mapping of Fe-TMC (spot 3). 44
Figure S45: Surface morphology and elemental composition of Fe-TMC (spot 3). 45
Figure S46: SEM-EDX mapping of Fe-TMC (spot 4). 46
Figure S47: Surface morphology and elemental composition of Fe-TMC (spot 4). 47
Figure S48: SEM-EDX mapping of Fe-TMC (spot 5). 48
Figure S49: Surface morphology and elemental composition of Fe-TMC (spot 5). 49

Phosphate and Arsenate Determination

Phosphate Determination

The equilibrium orthophosphate concentration in the solution was measured using A ready to use phosphate determination reagent (vanadate-molybdate reagent; Sigma-Aldrich) was used. An aliquot of the equilibrated orthophosphate solution was mixed with the vanadate-molybdate reagent and Millipore water to be developed for 30 minutes before measuring light absorbance using a Spectronic 200E spectrometer (Thermo Scientific, Waltham, MA, USA) at 720 nm.

Arsenate Determination

The equilibrium arsenate concentration in the solution was measured using a molybdate assay, prepared as follows: A 20mL batch of molybdate assay was made by mixing 4 mL 613 mM L-ascorbic solution, 4 mL 24 mM ammonium molybdate solution, 2 mL 8 mM Potassium antimony (II) tartrate solution and 10 mL 2.5M H_2SO_4 solution in order. An aliquot of the equilibrated arsenate solution was mixed with the molybdate assay and Millipore water to be developed for 30 minutes before measuring light absorbance using a Spectronic 200E spectrometer (Thermo Scientific, Waltham, MA, USA) at 900 nm.

FT-IR Spectroscopy

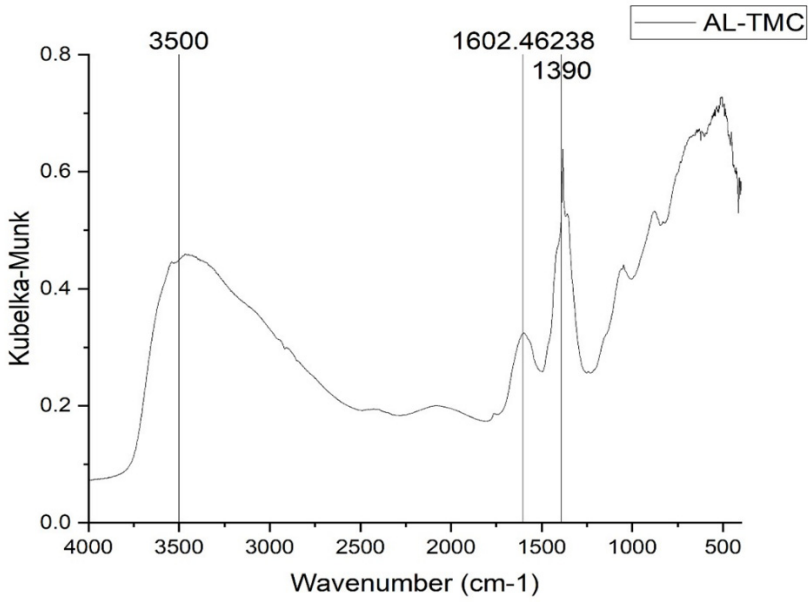

Figure S1: FT-IR spectrum of Al-TMC.

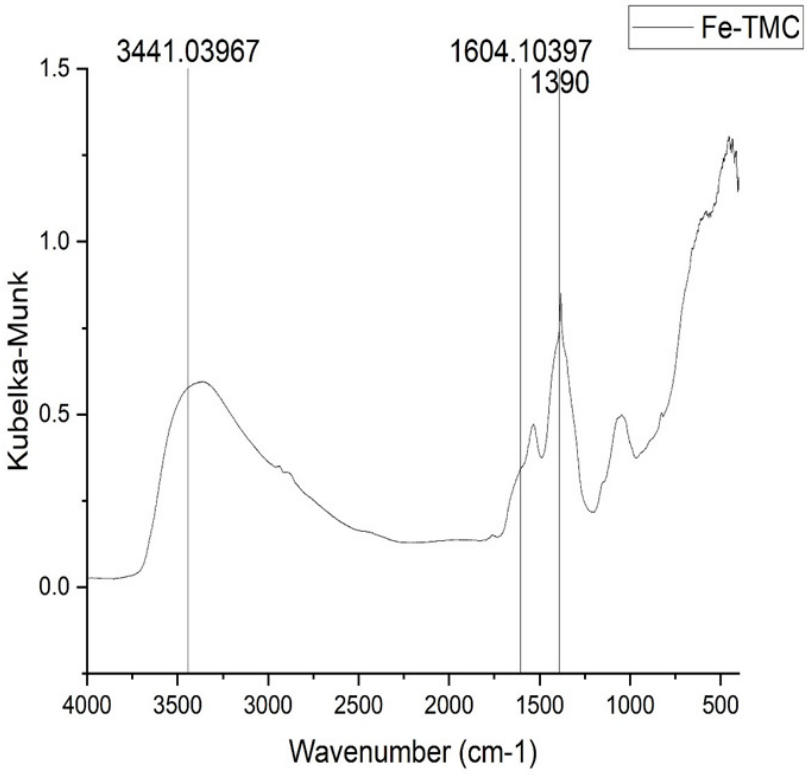

Figure S2: FT-IR spectrum of Fe-TMC.

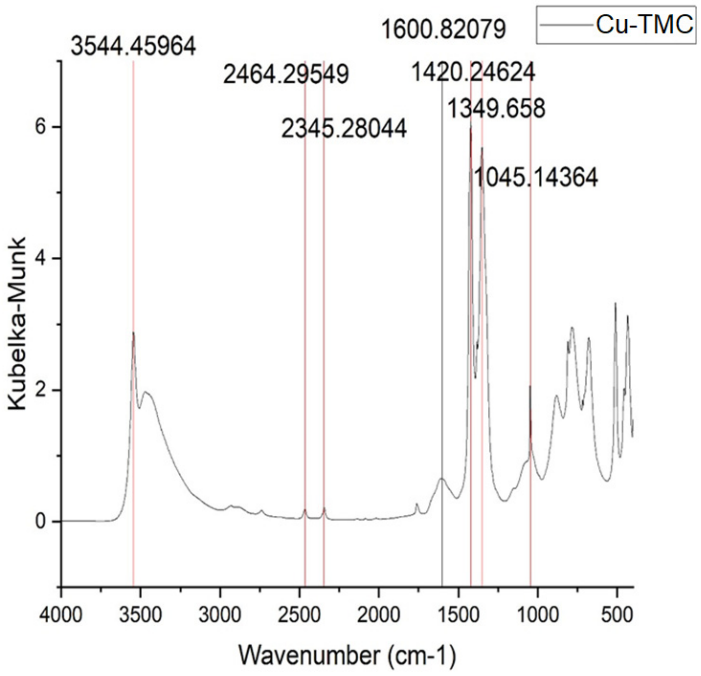

Figure S3: FT-IR spectrum of Cu-TMC.

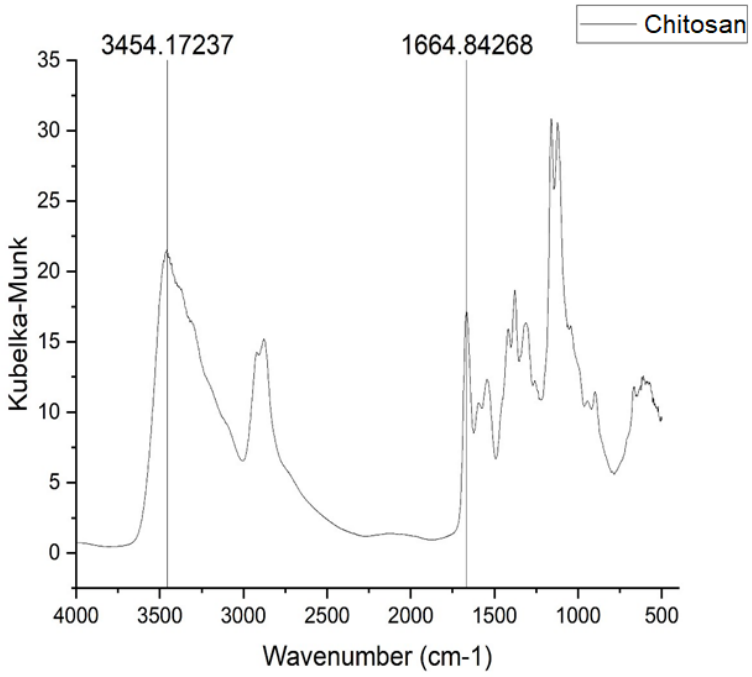

Figure S4: FT-IR spectrum of Chitosan.

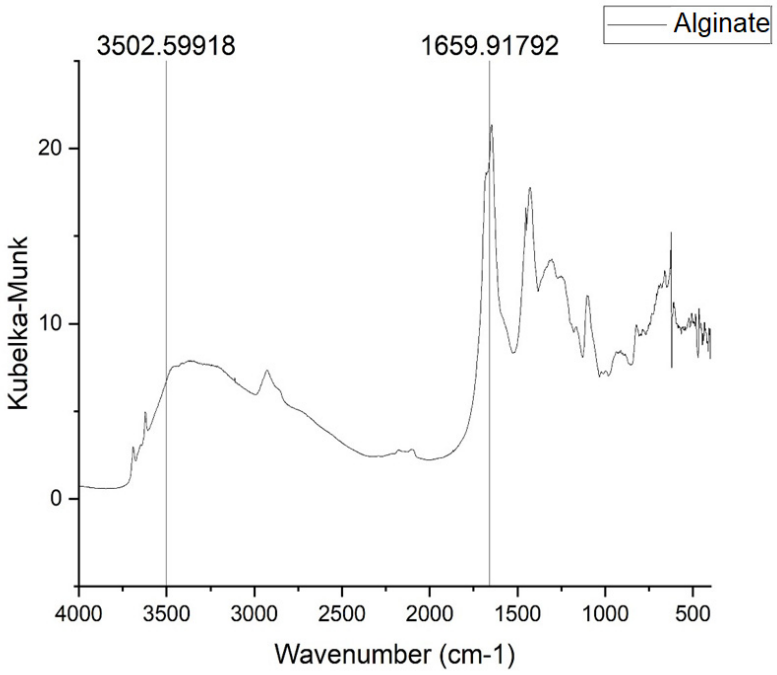

Figure S5: FT-IR spectrum of Sodium Alginate.

Point-of-Zero (PZC) Determination

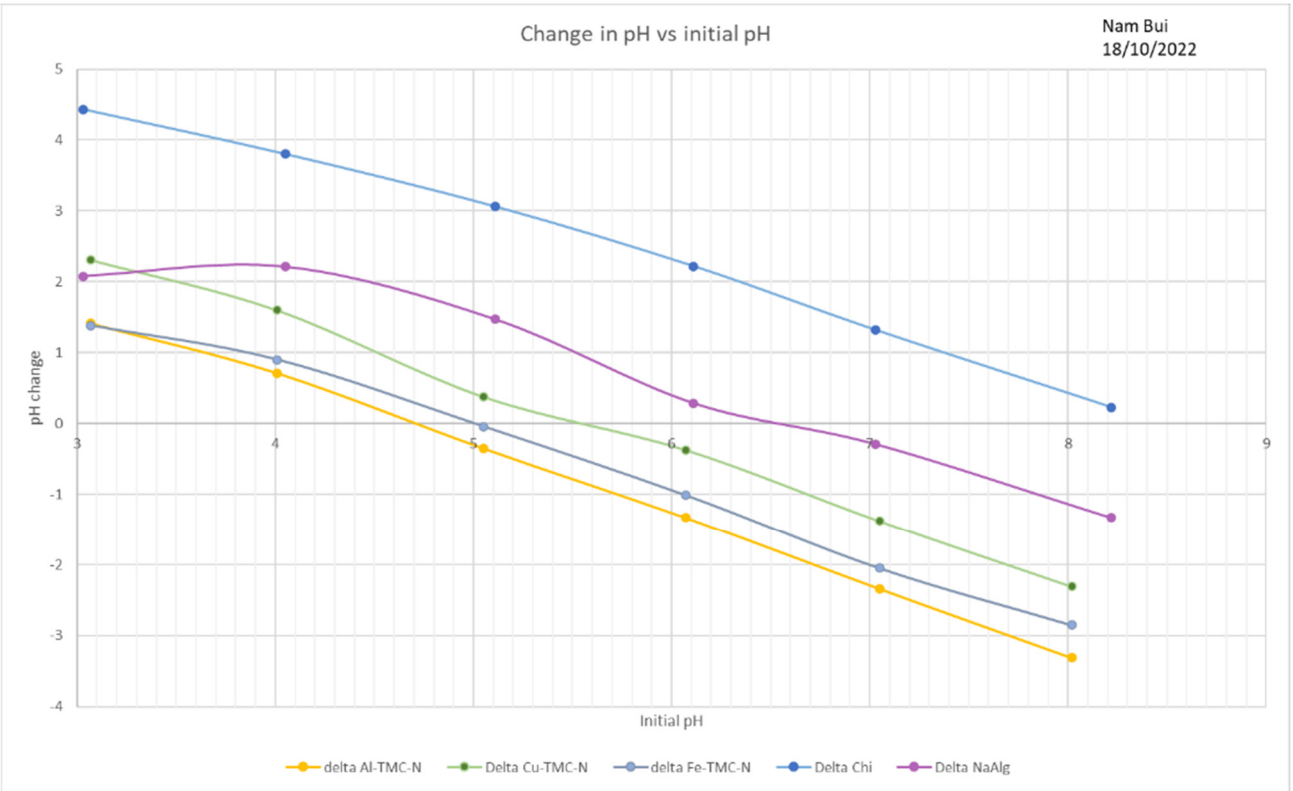

Figure S6: Change in pH vs initial pH plot.

Table S1: Results of the pH measurements to determine the PZC.

pHi	Al-TMC	Cu-TMC	Fe-TMC	NaAlg
3.07	4.48	5.38	4.45	5.11
4.01	4.72	5.61	4.91	6.26
5.05	4.7	5.43	5.01	6.58
6.07	4.74	5.7	5.06	6.4
7.05	4.71	5.67	5	6.74
8.02	4.71	5.71	5.17	6.89
9.07	4.83	5.56	5.05	

Table S2: Tabled ΔpH values and initial pH values used for PZC calculations.

pHi	ΔpH Al-TMC	ΔpH Cu-TMC	ΔpH Fe-TMC	ΔpH NaAlg	ΔpH Chi	pHi Chi Naalg
3.07	1.41	2.31	1.38	2.08	4.43	3.03
4.01	0.71	1.6	0.9	2.21	3.8	4.05
5.05	-0.35	0.38	-0.04	1.47	3.06	5.11
6.07	-1.33	-0.37	-1.01	0.29	2.22	6.11
7.05	-2.34	-1.38	-2.05	-0.29	1.32	7.03
8.02	-3.31	-2.31	-2.85	-1.33	0.23	8.22
PZC	4.7	5.55	5.6	6.6	8.4	

Phosphate adsorption at pH 6.3

Table S3: Isotherm parameters fit with Sips model for phosphate adsorption at pH 6.3 at 22 ˚C.

Adsorbate: Phosphate			
Adsorbent	**Al TMC**	**Fe TMC**	**Cu TMC**
Q_{max} (mg/g)	93	77	17
K	0.90	0.28	0.36
Adjusted R^2	0.77	0.96	0.79
n	0.82	0.28	1.2

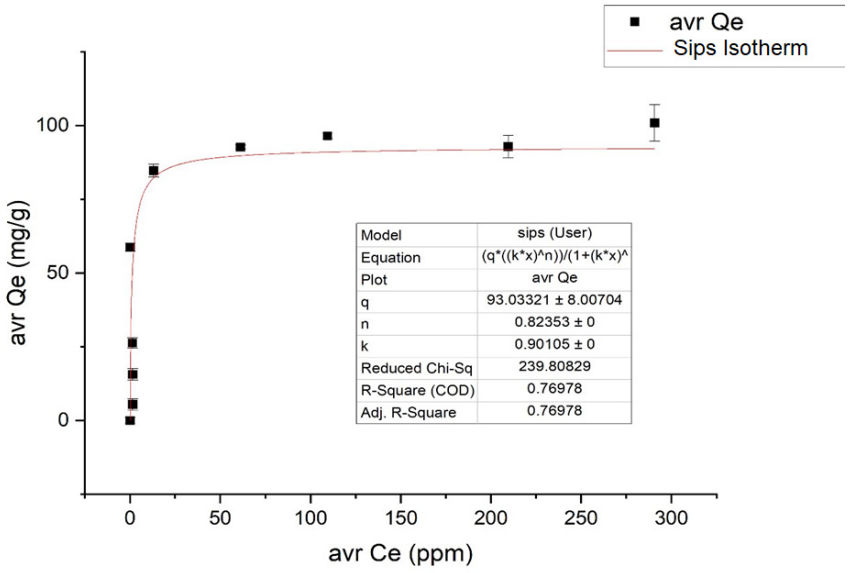

Figure S7: Phosphate adsorption at pH 6.3 isotherm of Al-TMC.

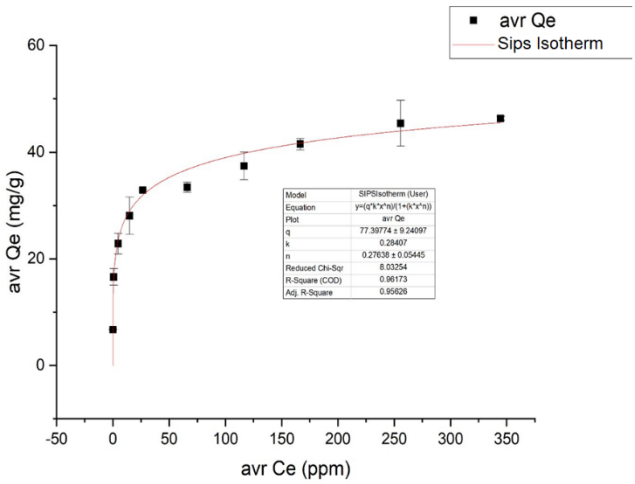

Figure S8: Phosphate adsorption at pH 6.3 isotherm of Fe-TMC.

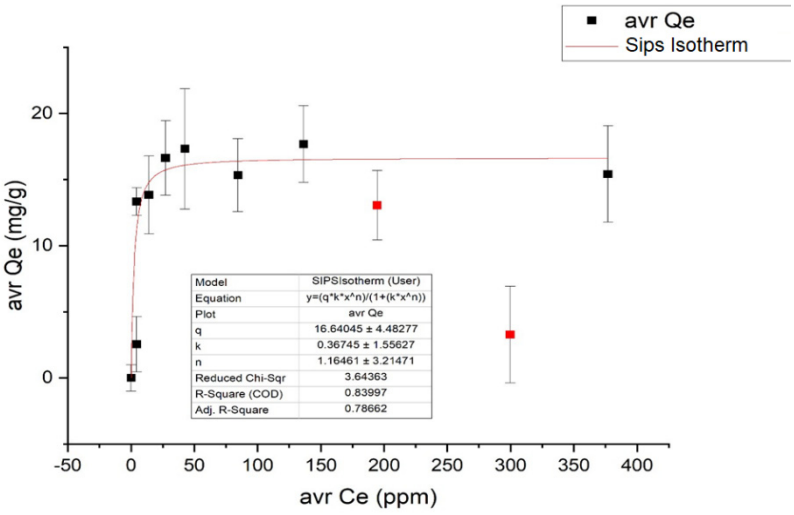

Figure S9:Phosphate adsorption at pH 6.3 isotherm of Cu-TMC.

Arsenate adsorption isotherms at pH 6.7

Table S4: Isotherm parameters fit with Sips model for arsenate adsorption at pH 6.7 at 22˚C

Adsorbate: Arsenate

Adsorbent	Al TMC	Fe TMC	Cu TMC
Q_{max} (mg/g)	80	66	31
K	14.7	0.57	2.58E-5
Adjusted R^2	0.85	0.99	0.98
n	0.18	0.38	2.72

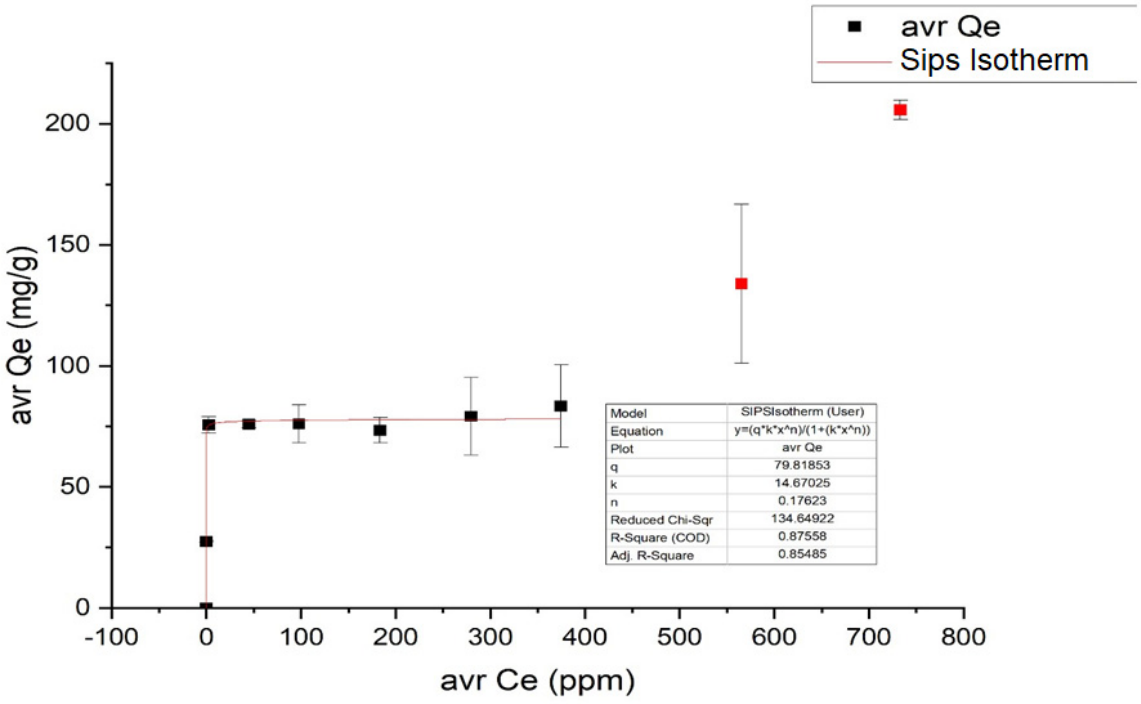

Figure S10: Arsenate adsorption isotherm of Al-TMC.

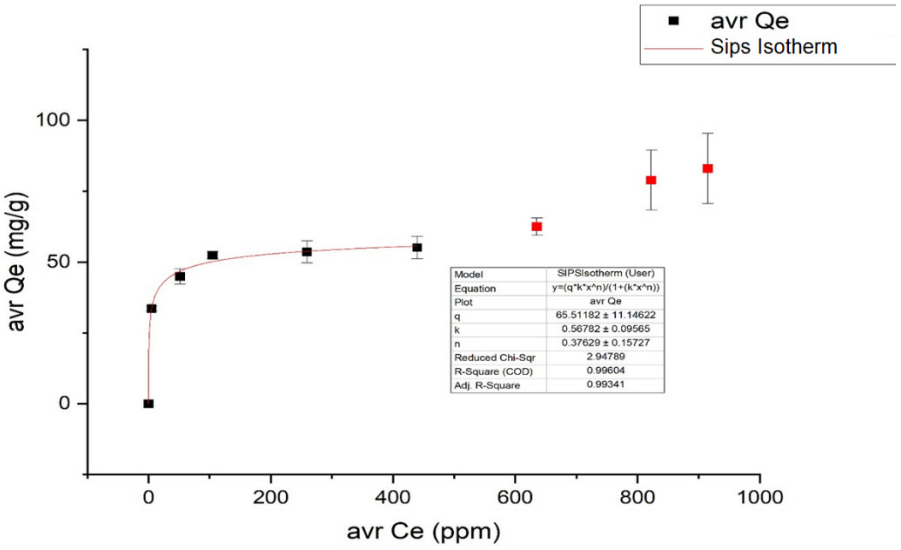

Figure S11: Arsenate adsorption isotherm of Fe-TMC.

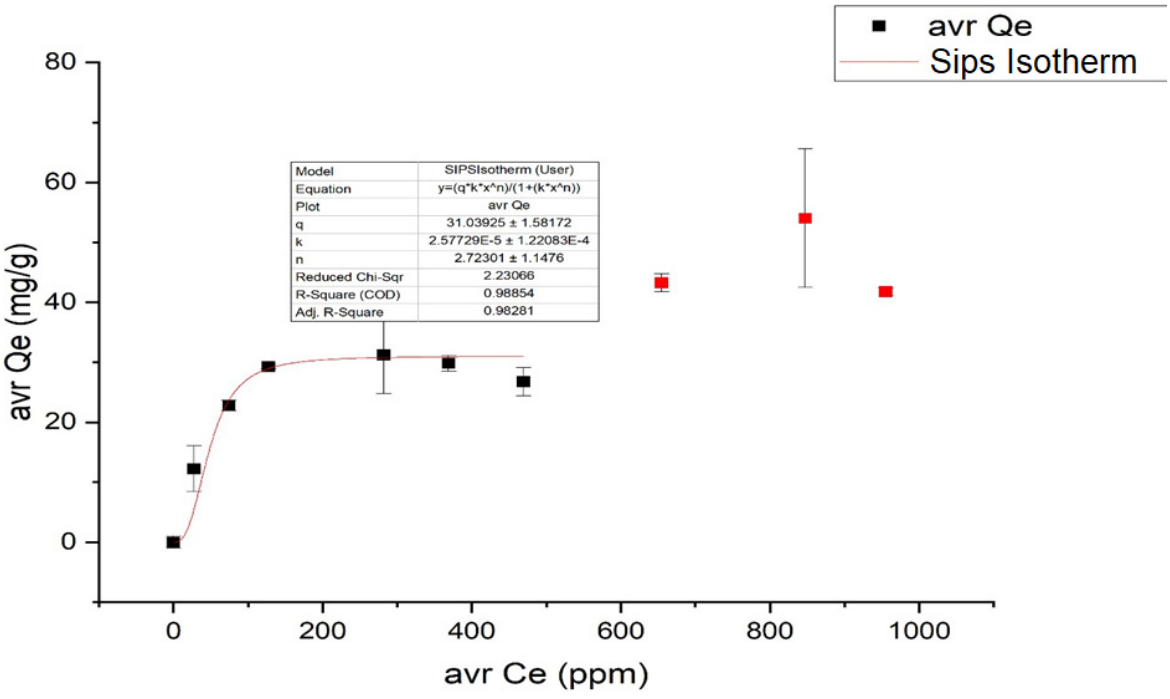

Figure S12: Arsenate adsorption isotherm of Al-TMC.

Phosphate adsorption Isotherms at pH 8.5

Table S5: Isotherm parameters fit with Sips model for phosphate adsorption at pH 8.5 at 22˚C

Adsorbate: Phosphate			
Adsorbent	**Al TMC**	**Fe TMC**	**Cu TMC**
Q_{max} (mg/g)	62	21	23
K	3.90	0.01	9.3E-3
Adjusted R^2	0.88	0.98	0.94
n	0.95	2.81	3.02

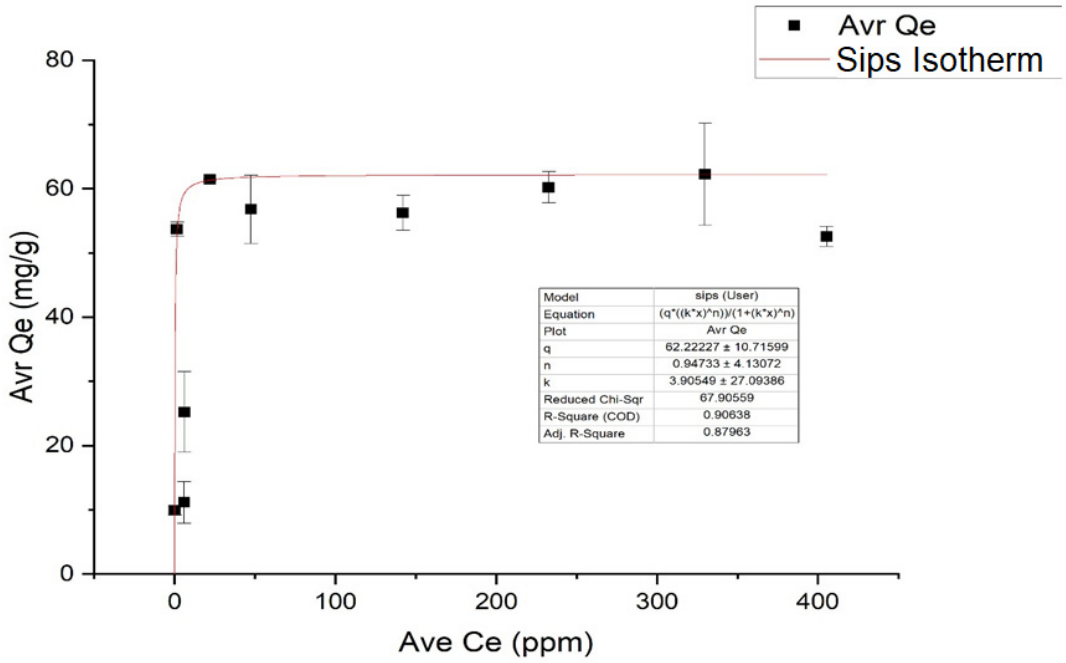

Figure S13: Phosphate adsorption at pH 8.5 isotherm of Al-TMC.

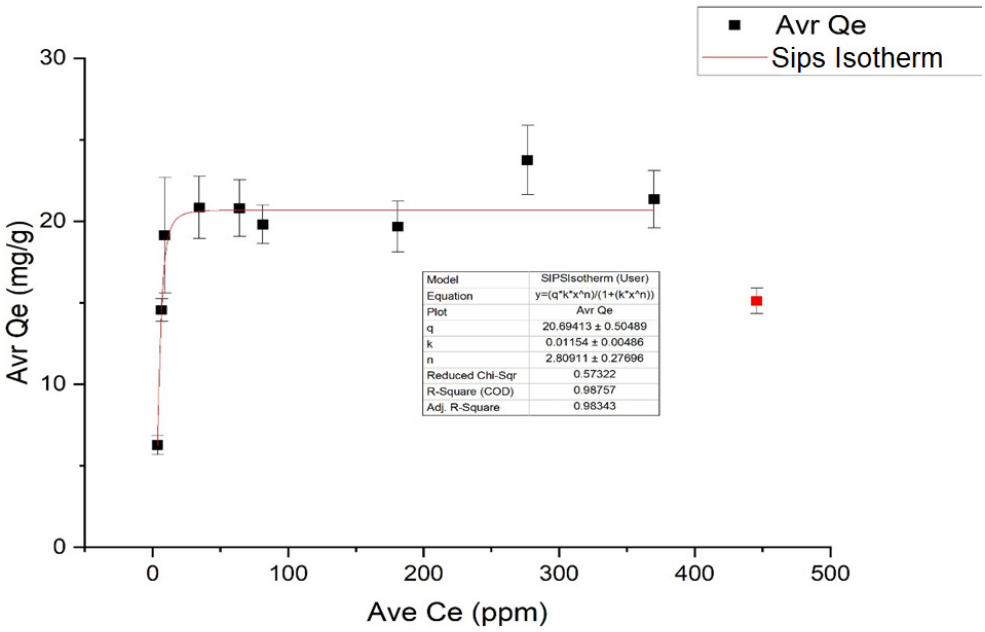

Figure S14: Phosphate adsorption at pH 8.5 isotherm of Fe-TMC.

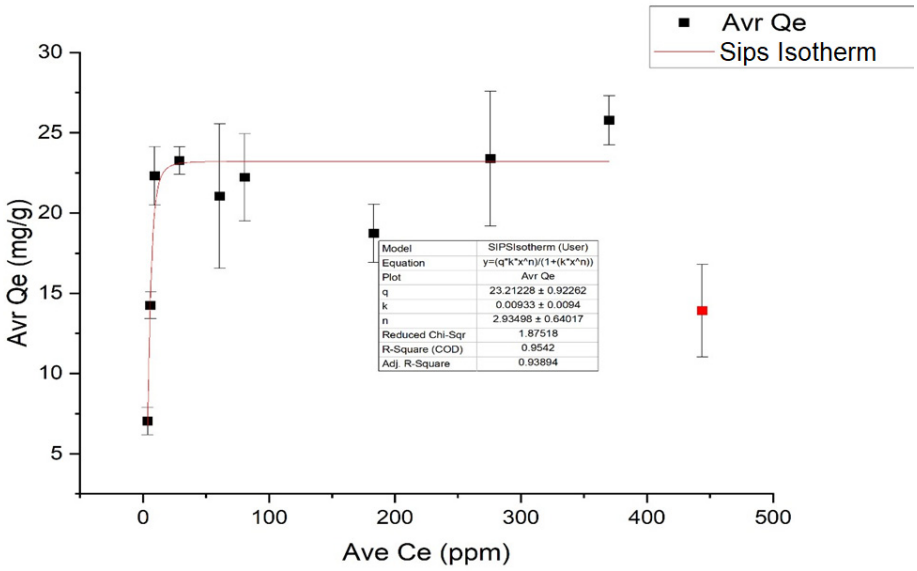

Figure S15: Phosphate adsorption at pH 8.5 isotherm of Cu-TMC.

SEM-EDX Imaging

Al-TMC
(Spot 1)

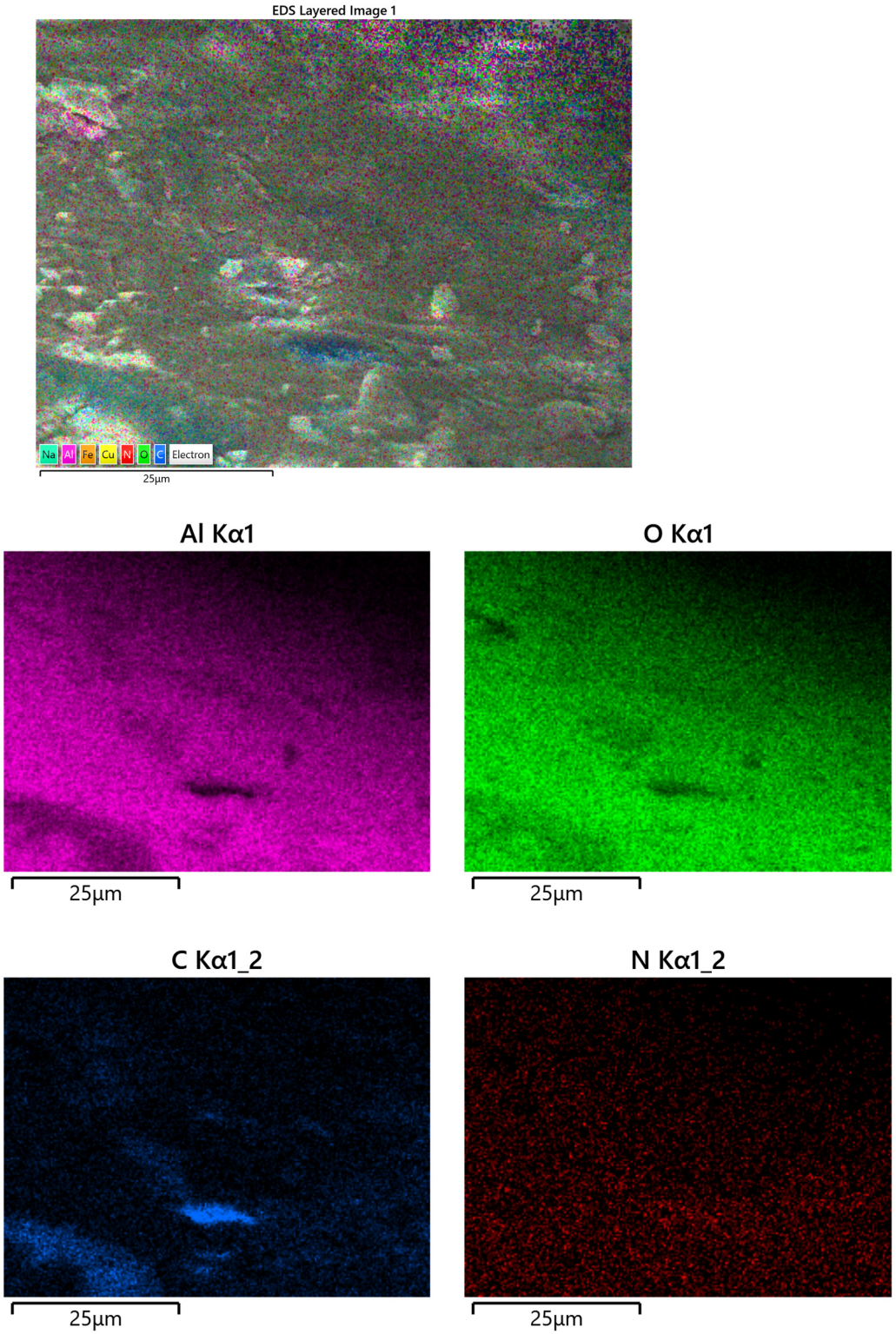

Figure S16: SEM-EDX mapping of Al-TMC (spot 1).

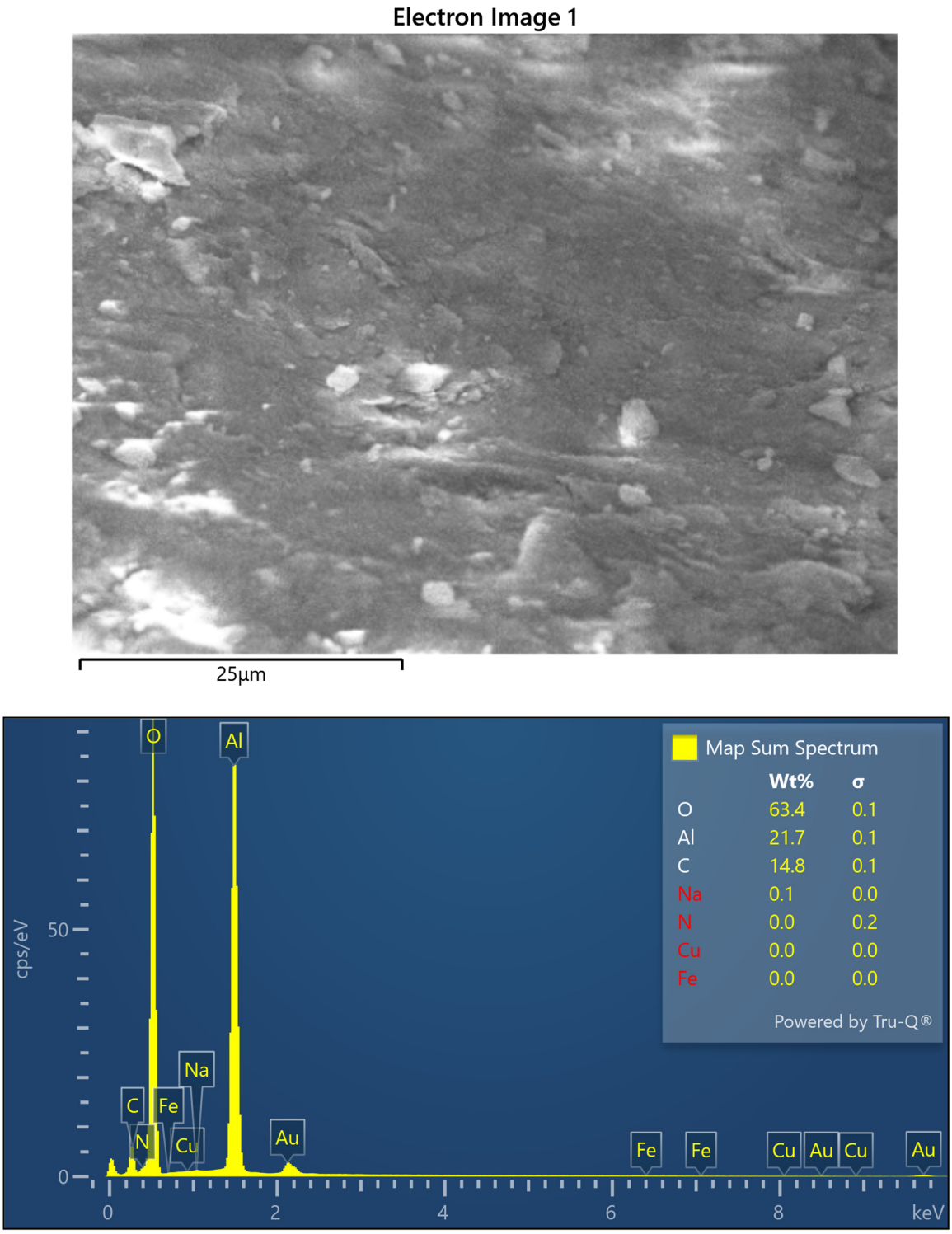

Figure S17: Surface morphology and elemental composition of Al-TMC (spot 1).

Spot 2

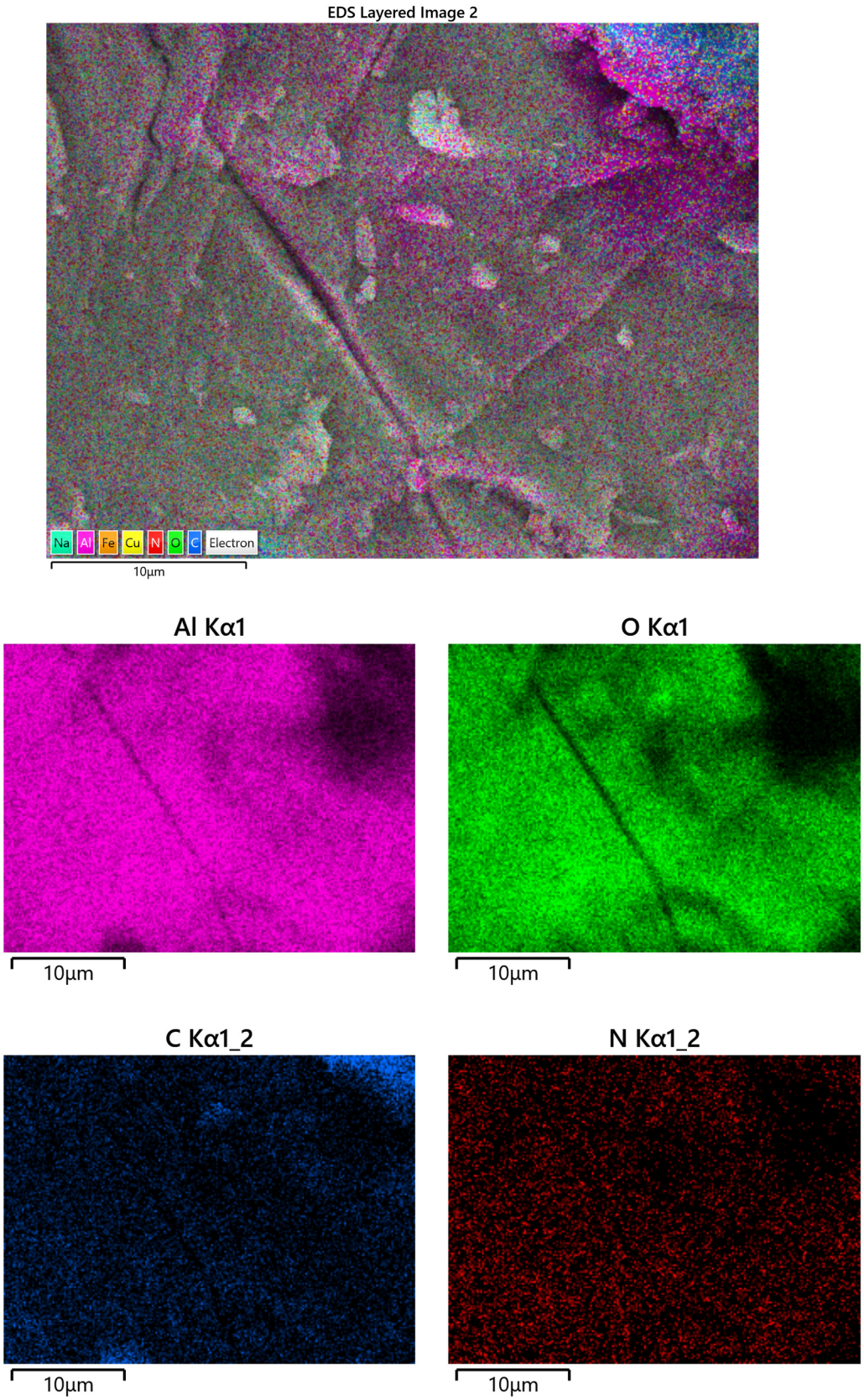

Figure S18: SEM-EDX mapping of Al-TMC (spot 2).

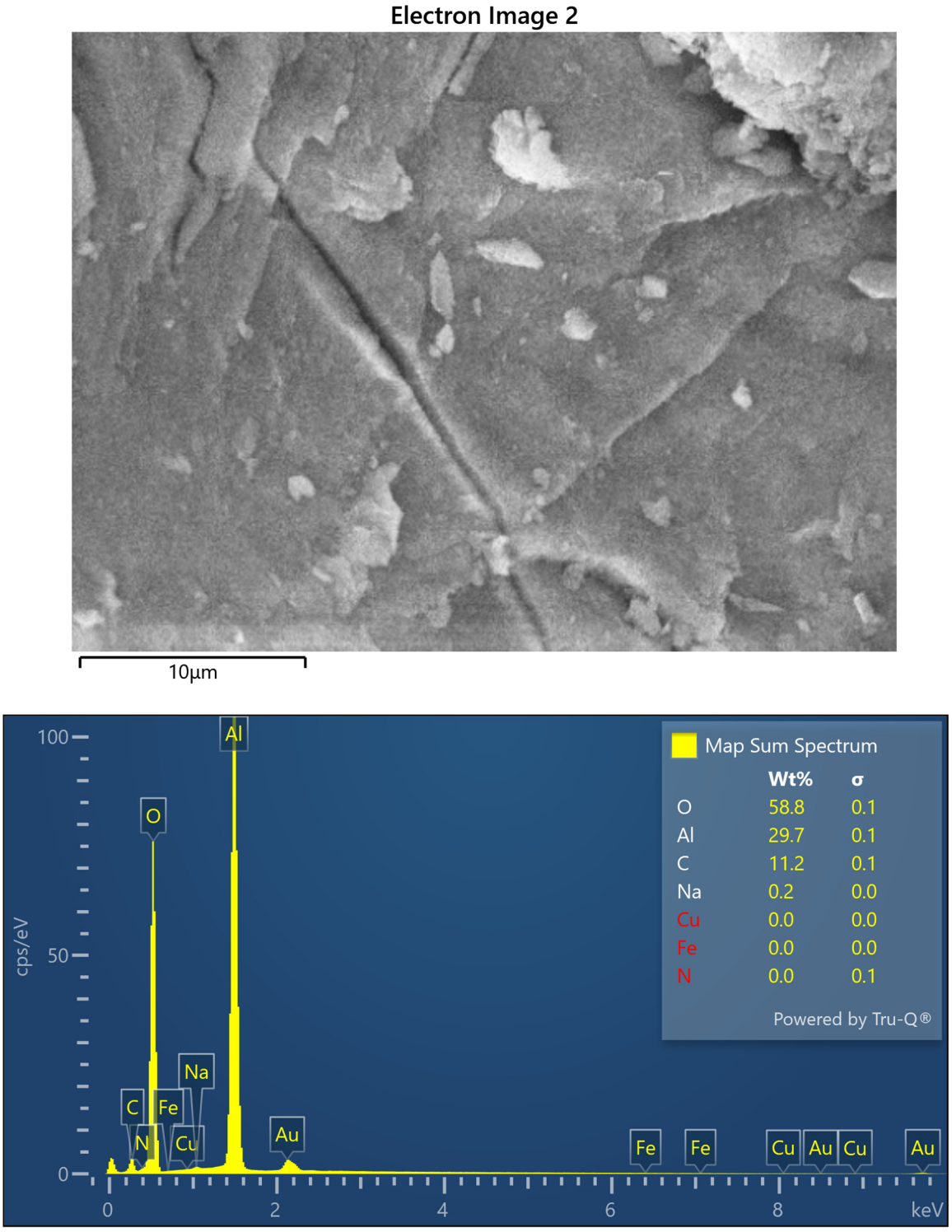

Figure S19: Surface morphology and elemental composition of Al-TMC (spot 2).

Spot 3

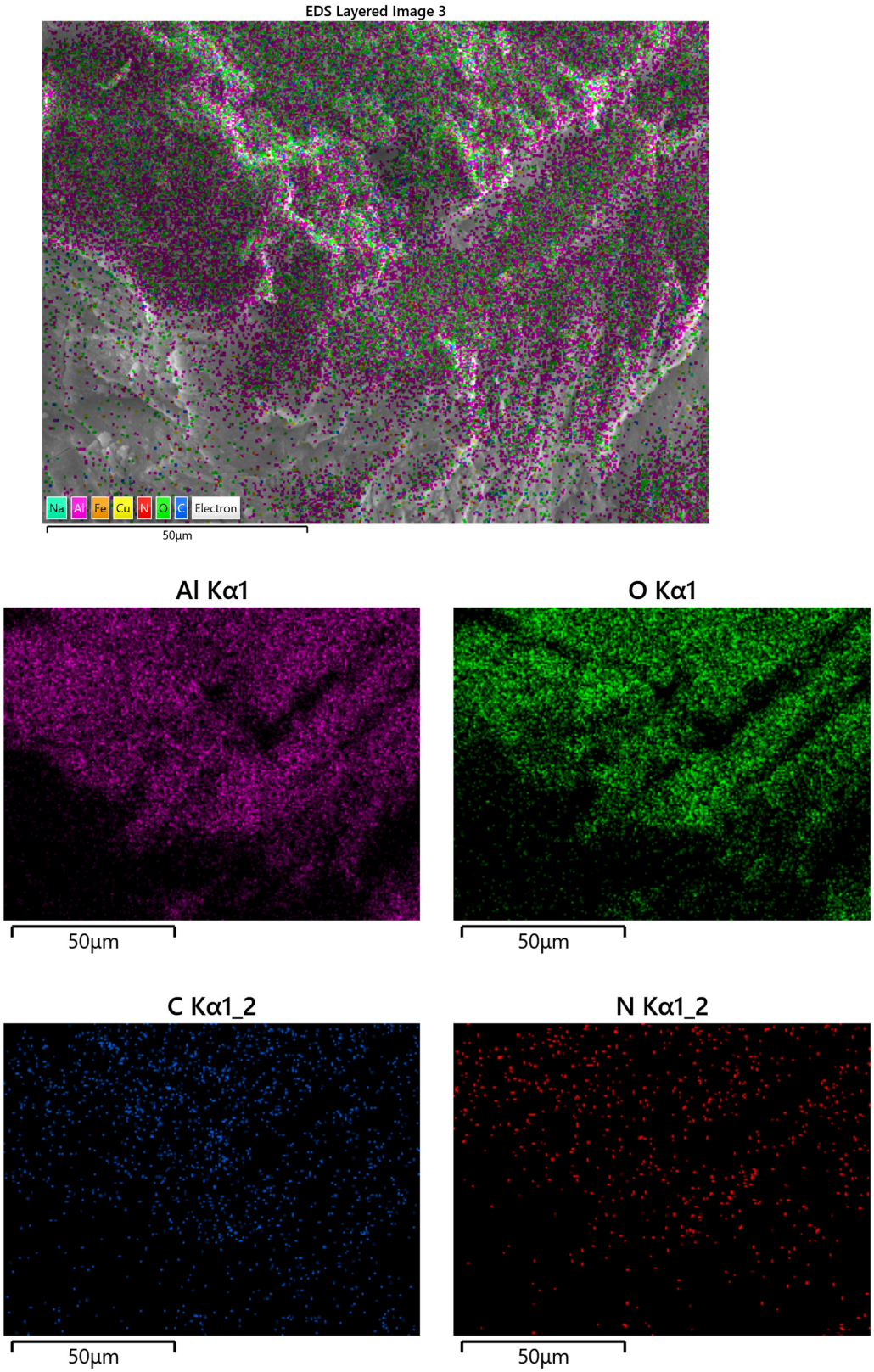

Figure S20: SEM-EDX mapping of Al-TMC (spot 3).

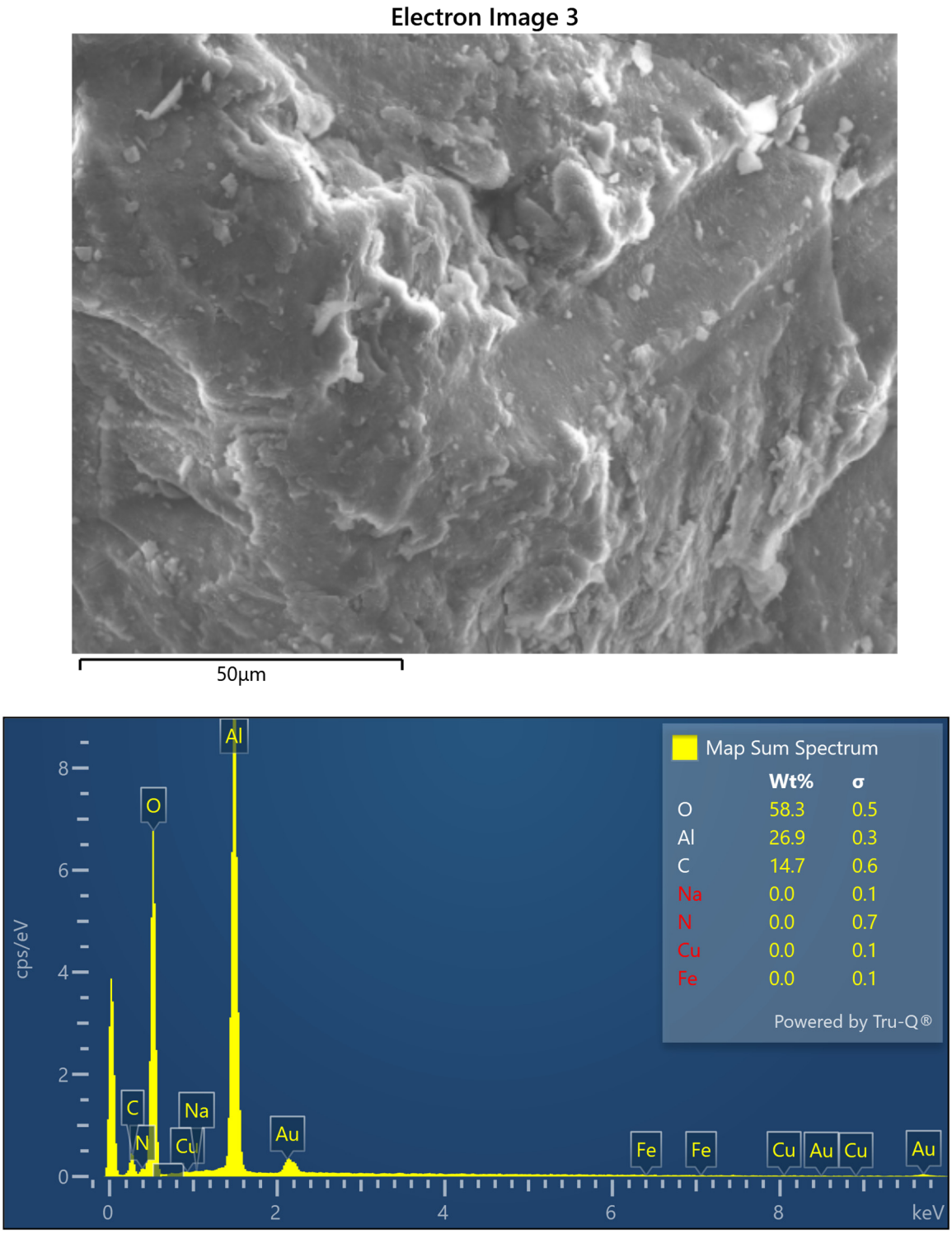

Figure S21: Surface morphology and elemental composition of Al-TMC (spot 3).

Spot 4

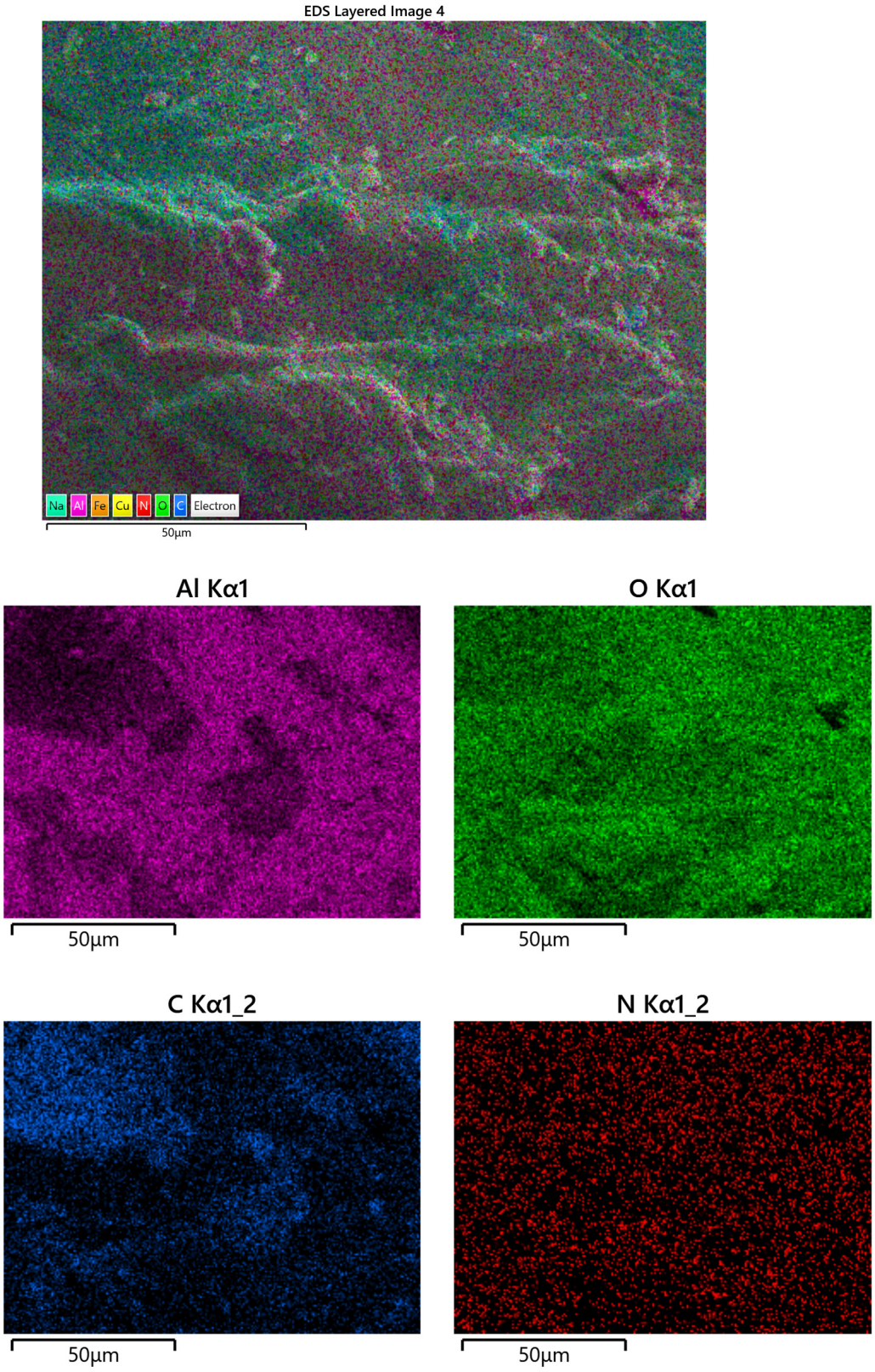

Figure S22: SEM-EDX mapping of Al-TMC (spot 4).

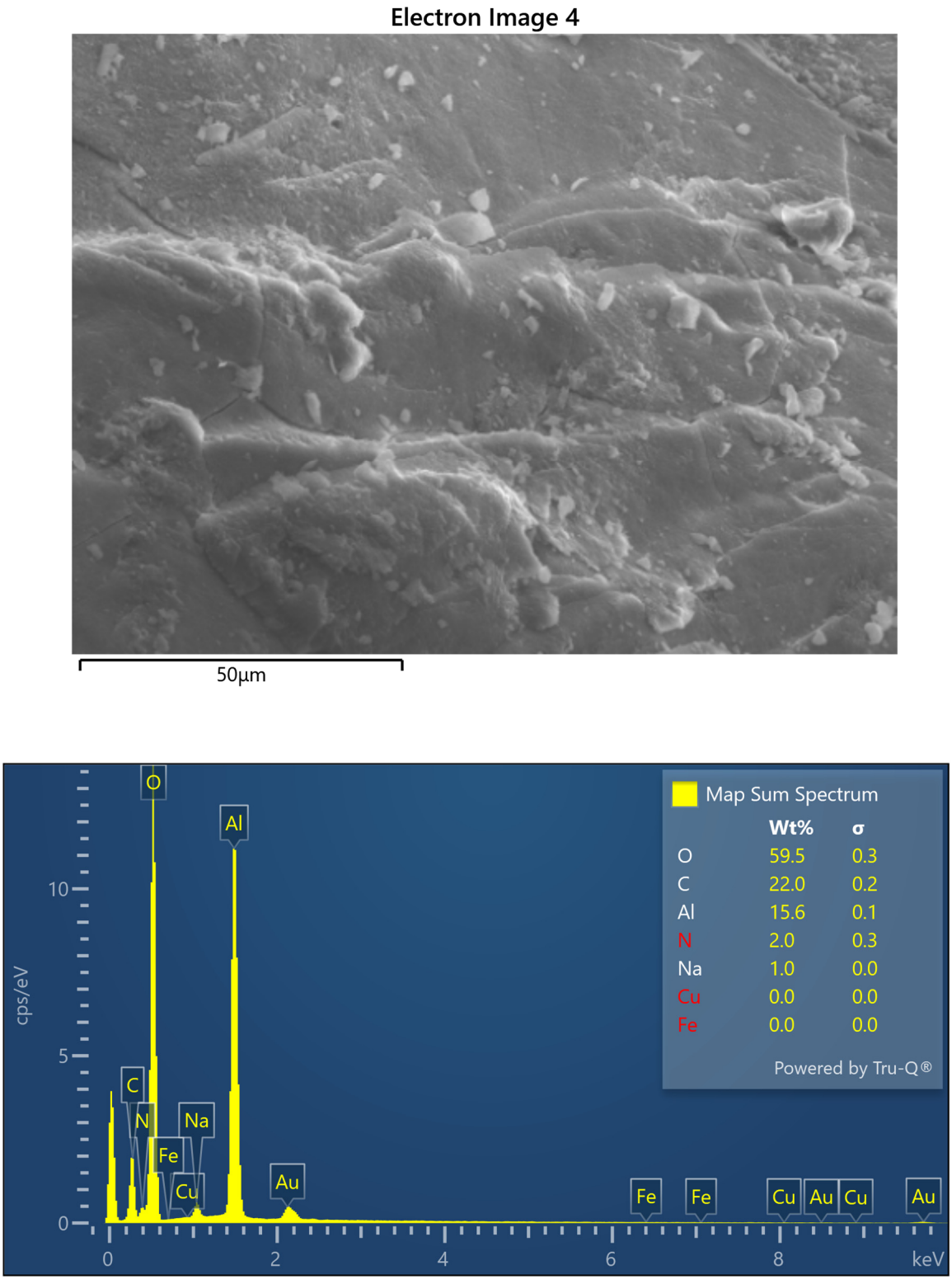

Figure S23: Surface morphology and elemental composition of Al-TMC (spot 4).

Spot 5

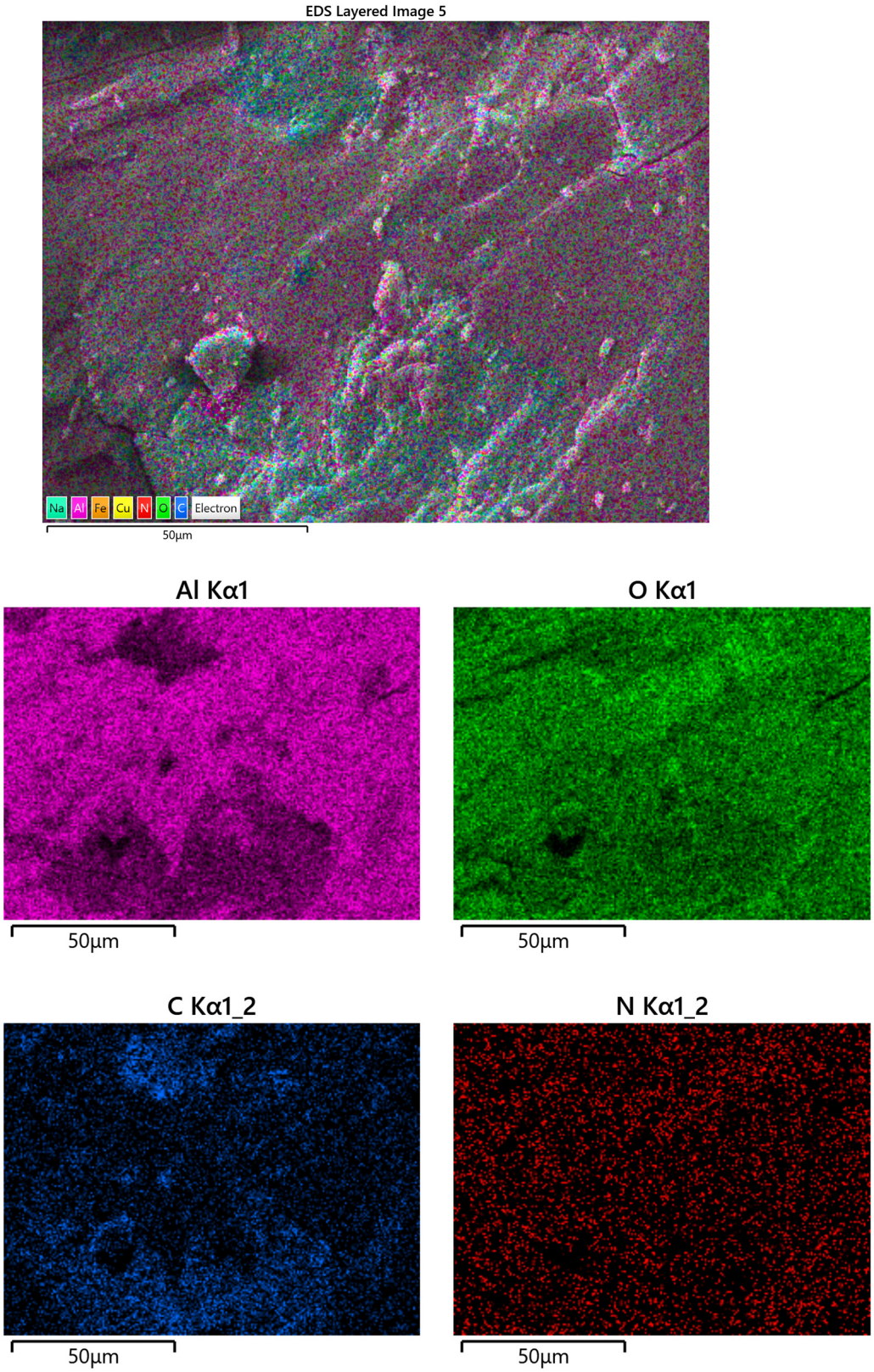

Figure S24: SEM-EDX mapping of Al-TMC (spot 5).

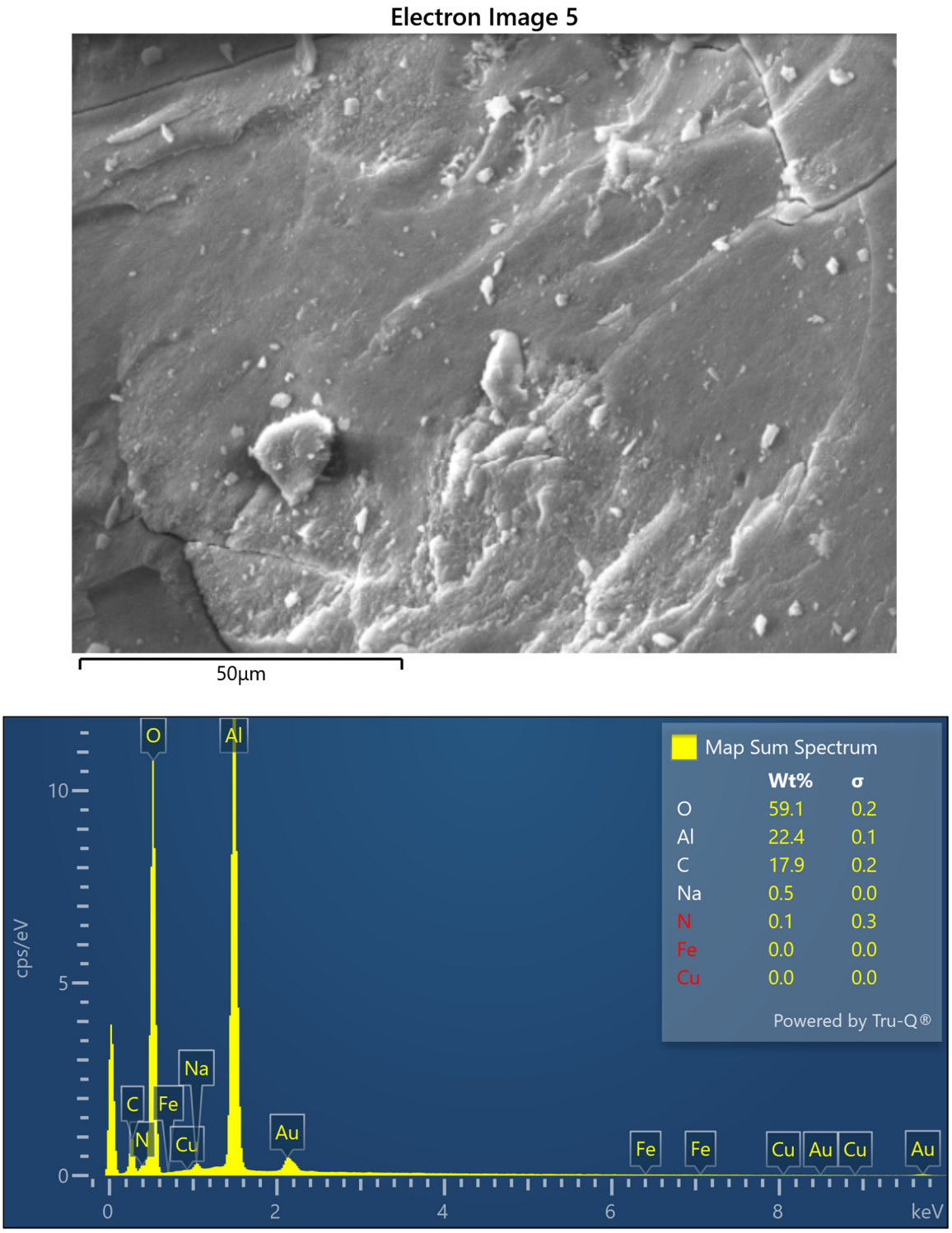

Figure S25: Surface morphology and elemental composition of Al-TMC (spot 5).

Spot 6

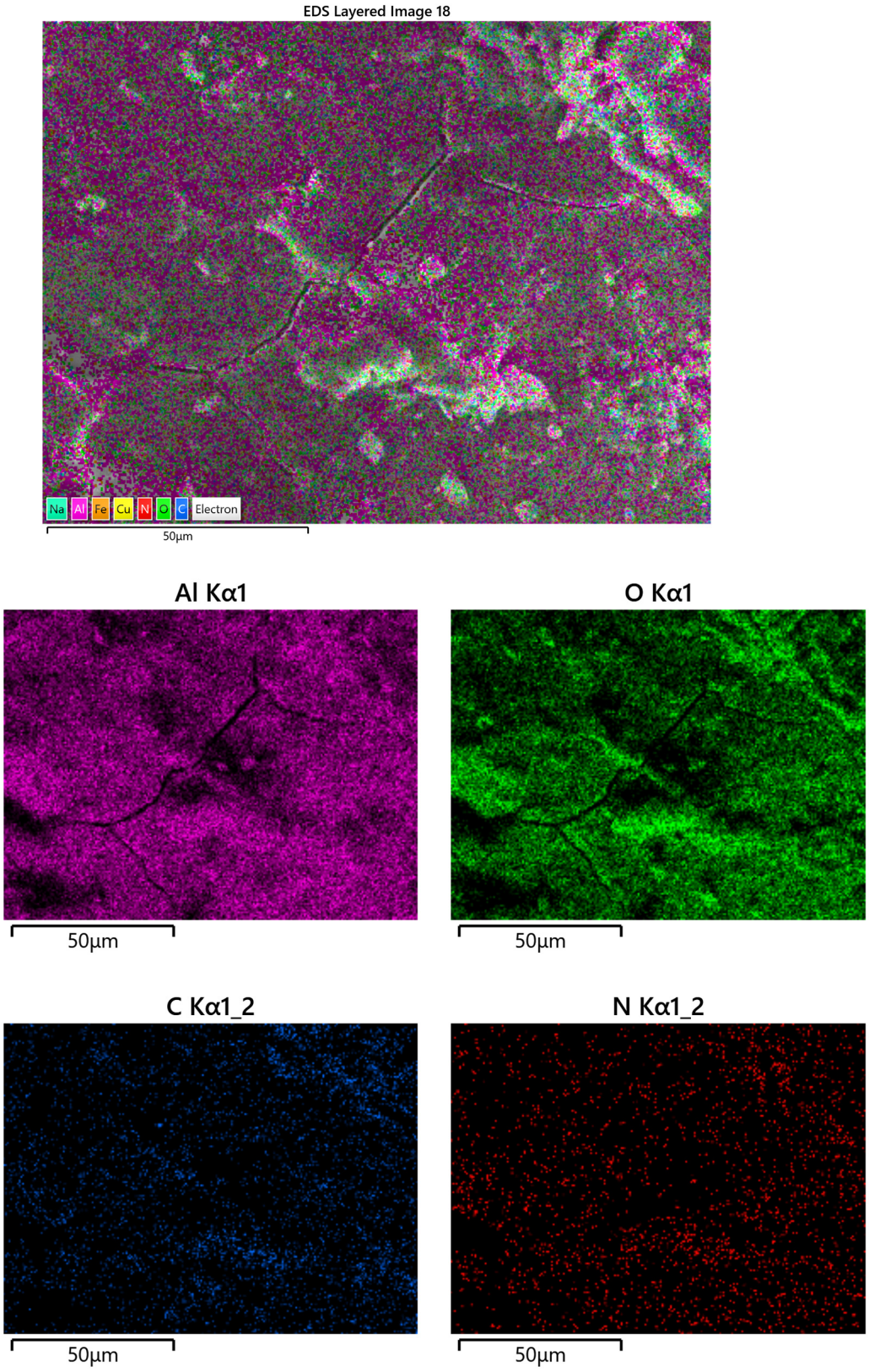

Figure S26: SEM-EDX mapping of Al-TMC (spot 6).

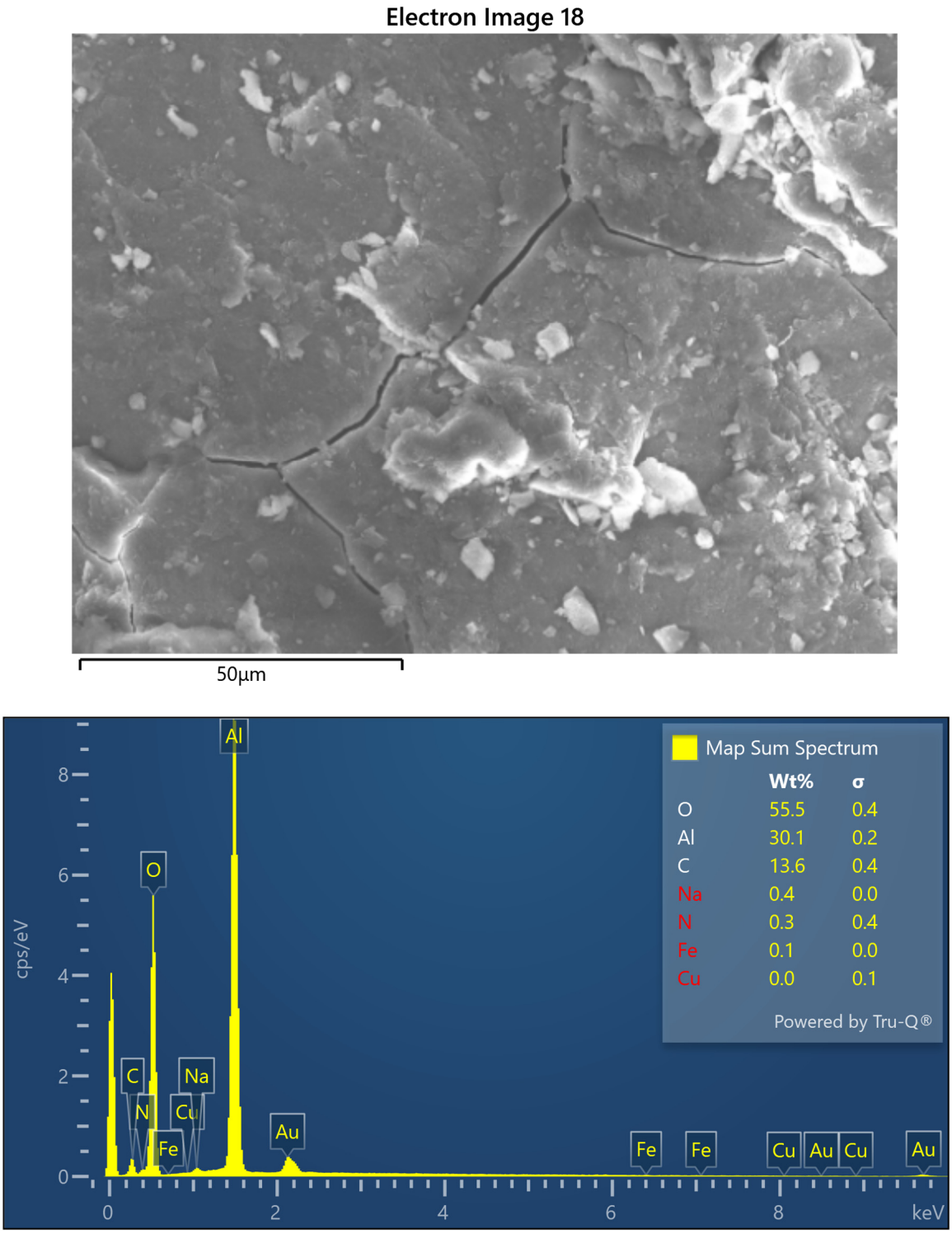

Figure S27: Surface morphology and elemental composition of Al-TMC (spot 6).

Cu-TMC
Spot 2

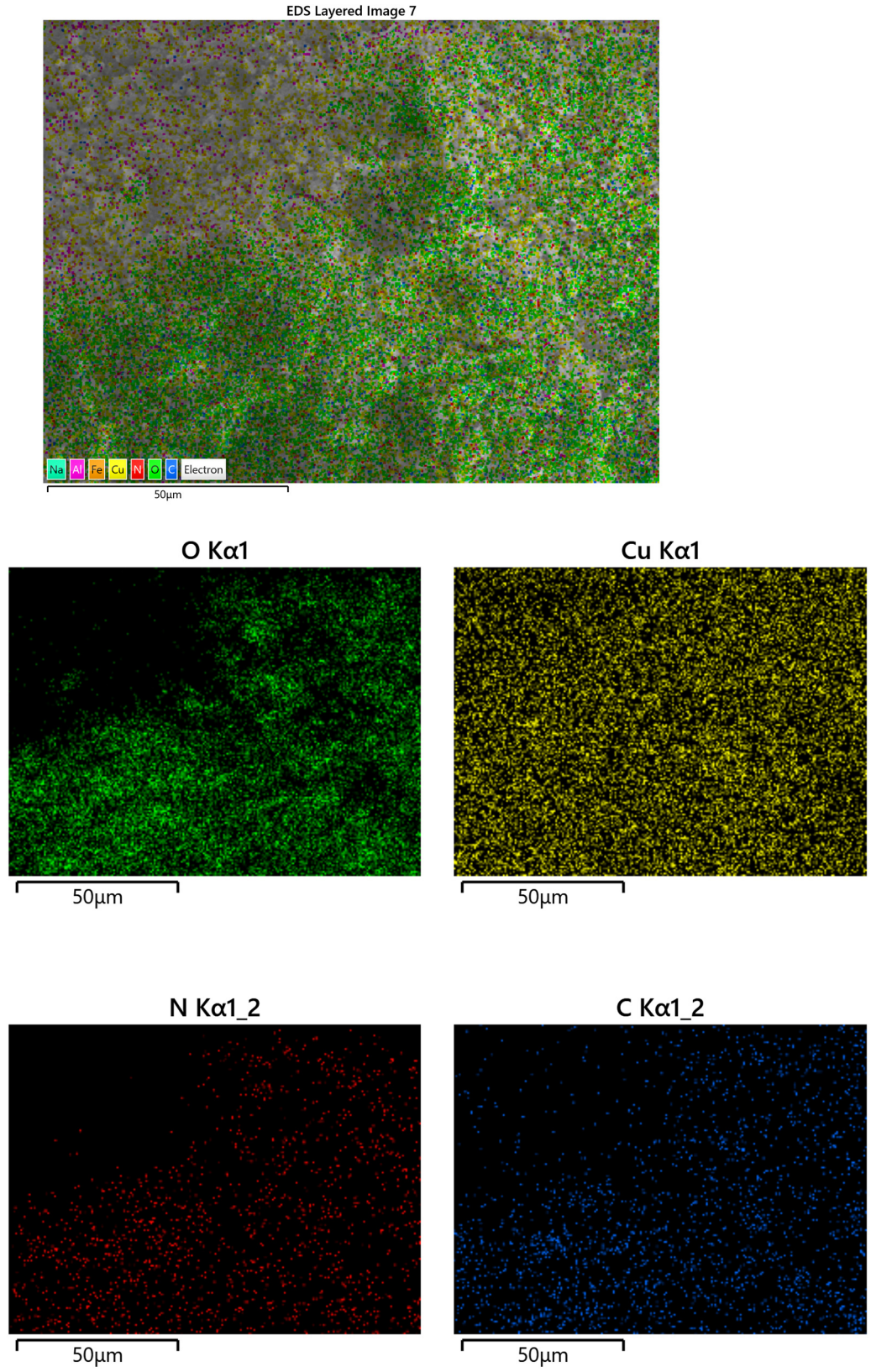

Figure S28: SEM-EDX mapping of Cu-TMC (spot 2).

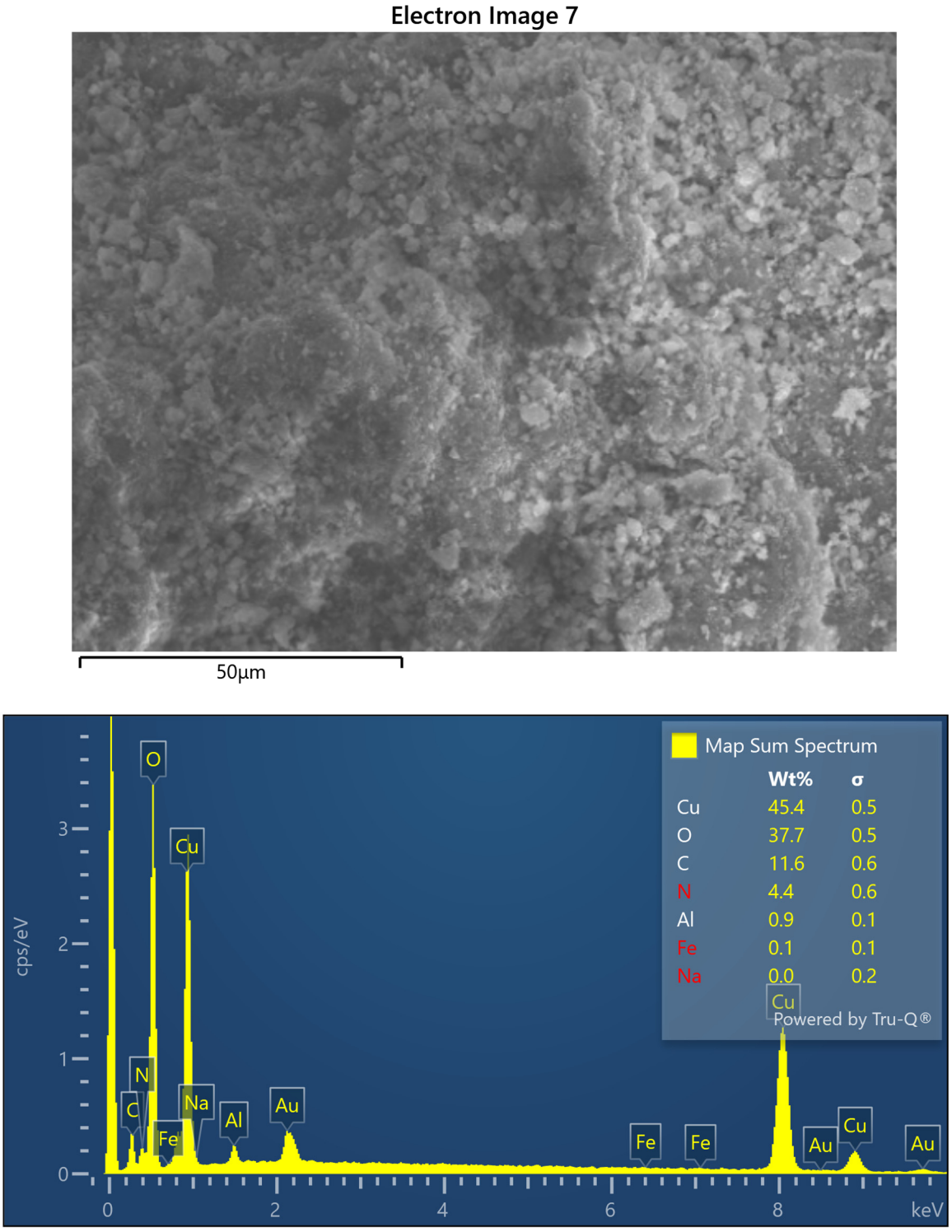

Figure S29: Surface morphology and elemental composition of Cu-TMC (spot 2).

Spot 3

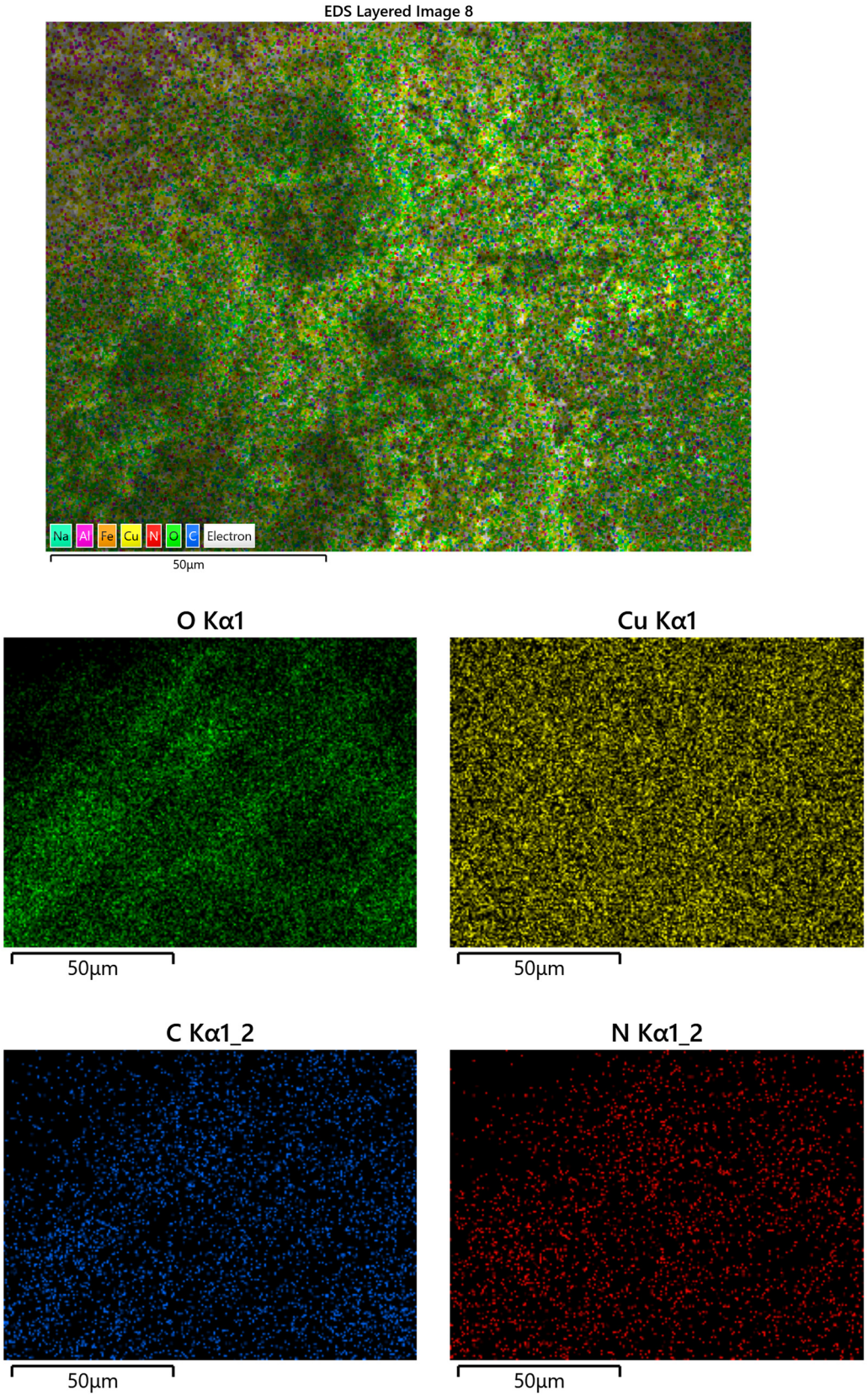

Figure S30: SEM-EDX mapping of Cu-TMC (spot 3).

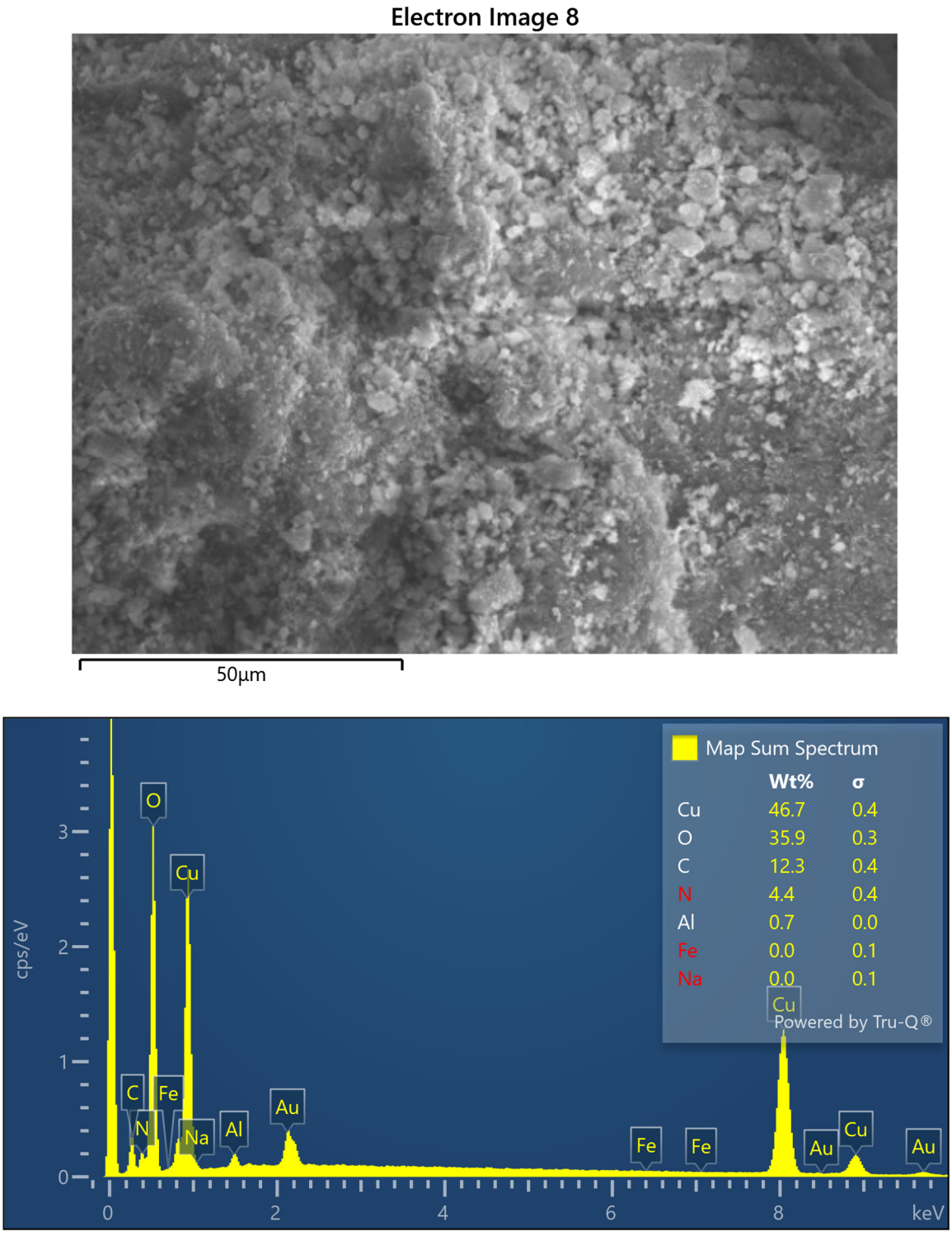

Figure S31: Surface morphology and elemental composition of Cu-TMC (spot 3).

Spot 4

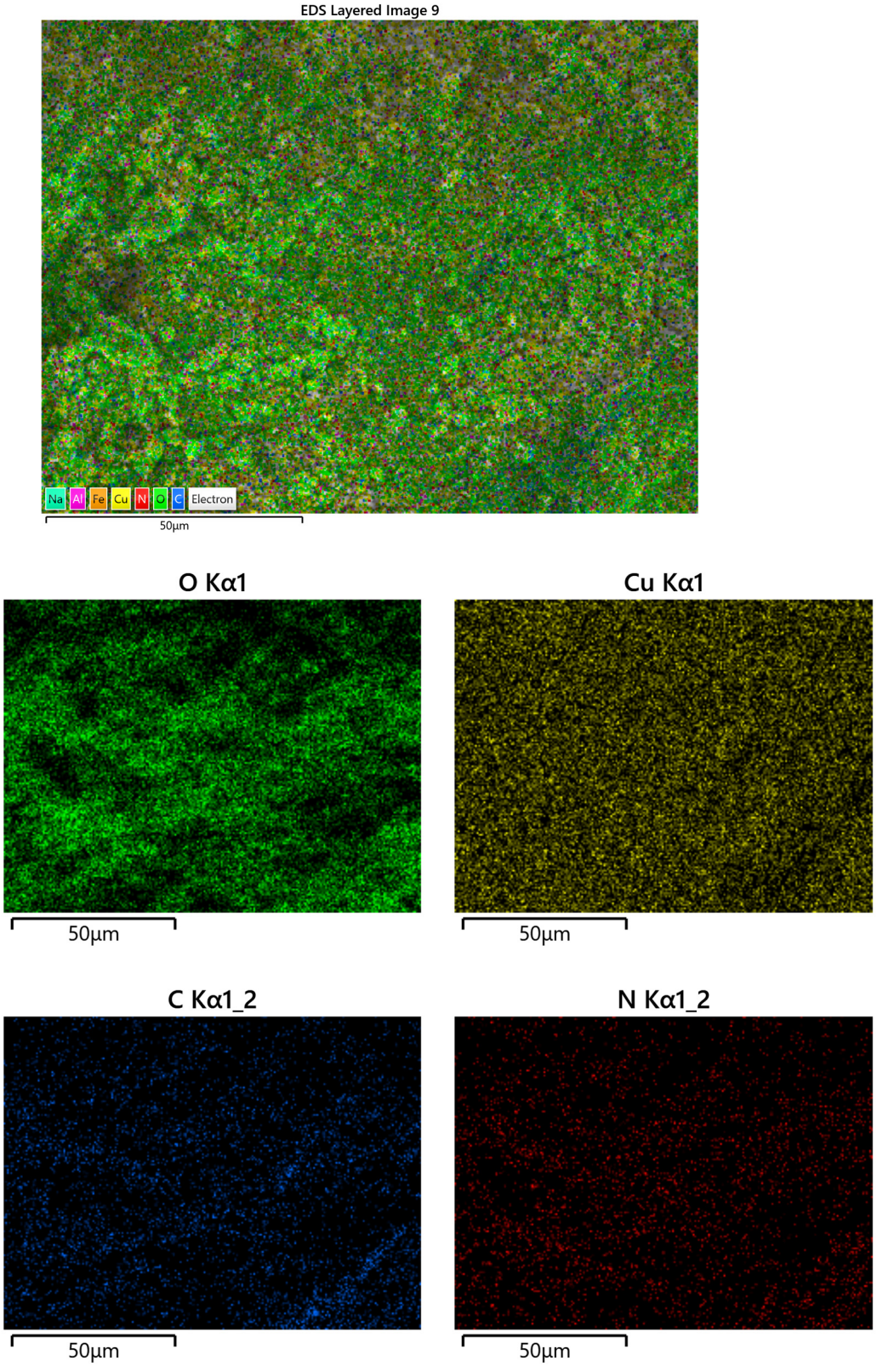

Figure S32: SEM-EDX mapping of Cu-TMC (spot 4).

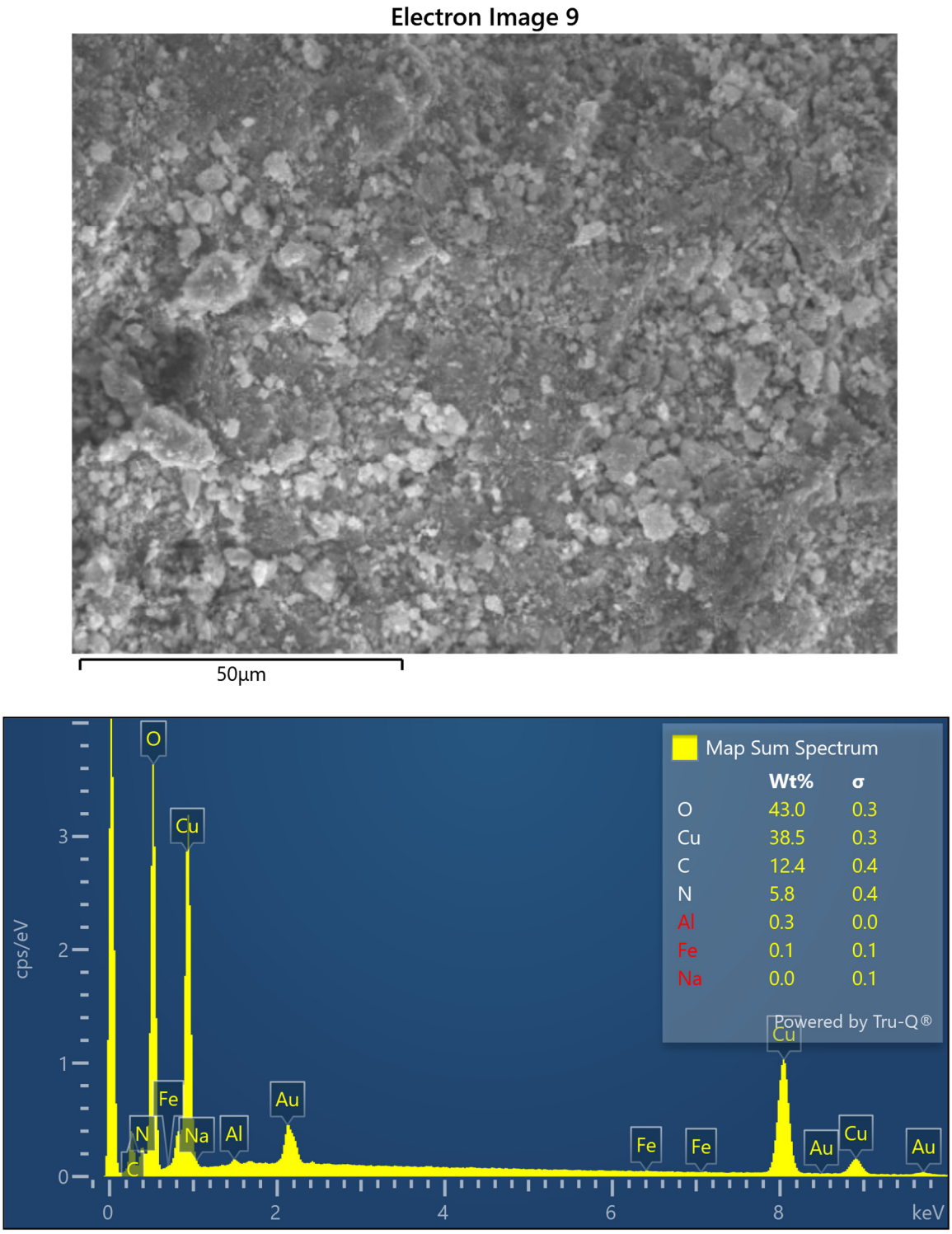

Figure S33: Surface morphology and elemental composition of Cu-TMC (spot 4).

Spot 5

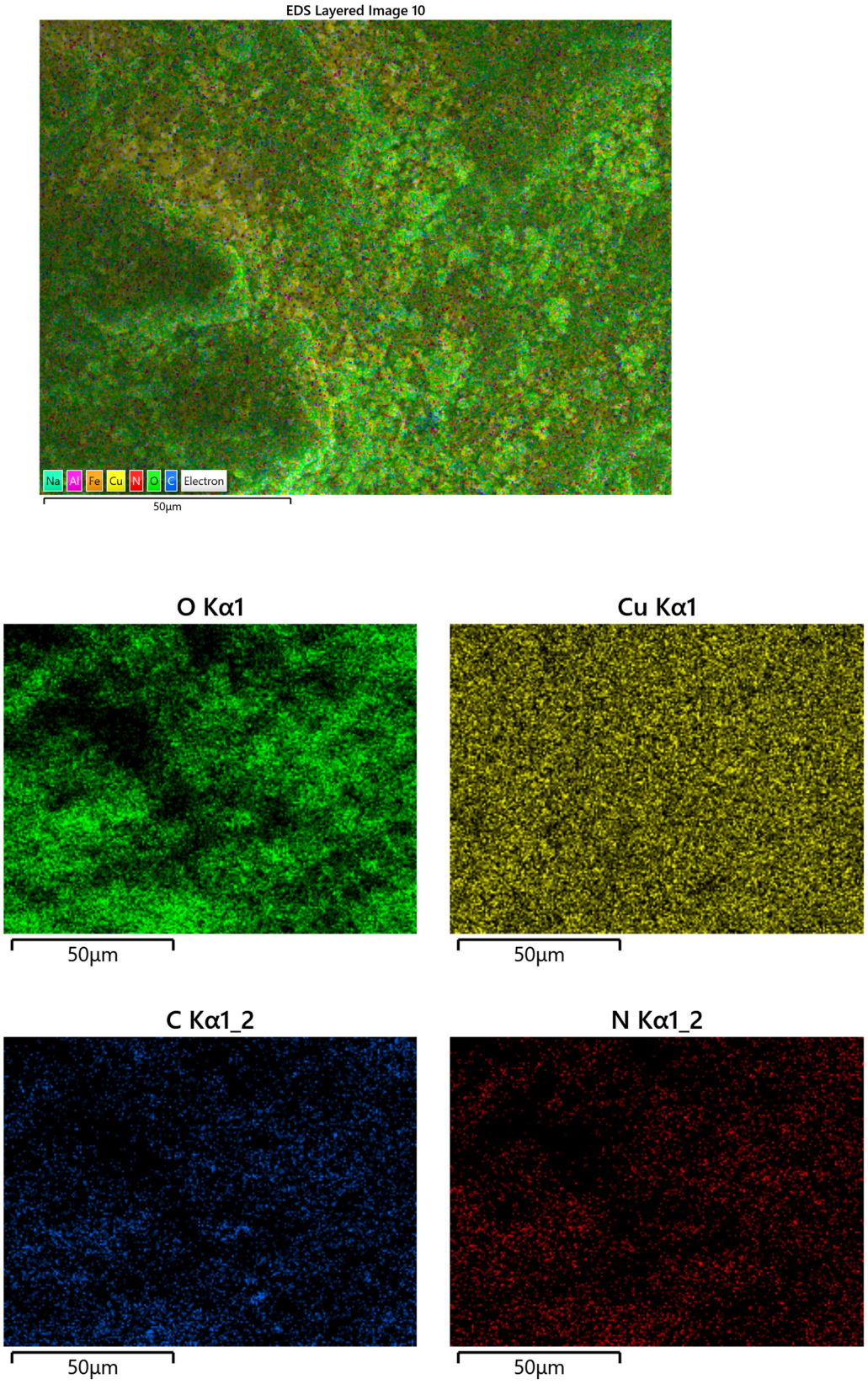

Figure S34: SEM-EDX mapping of Cu-TMC (spot 5).

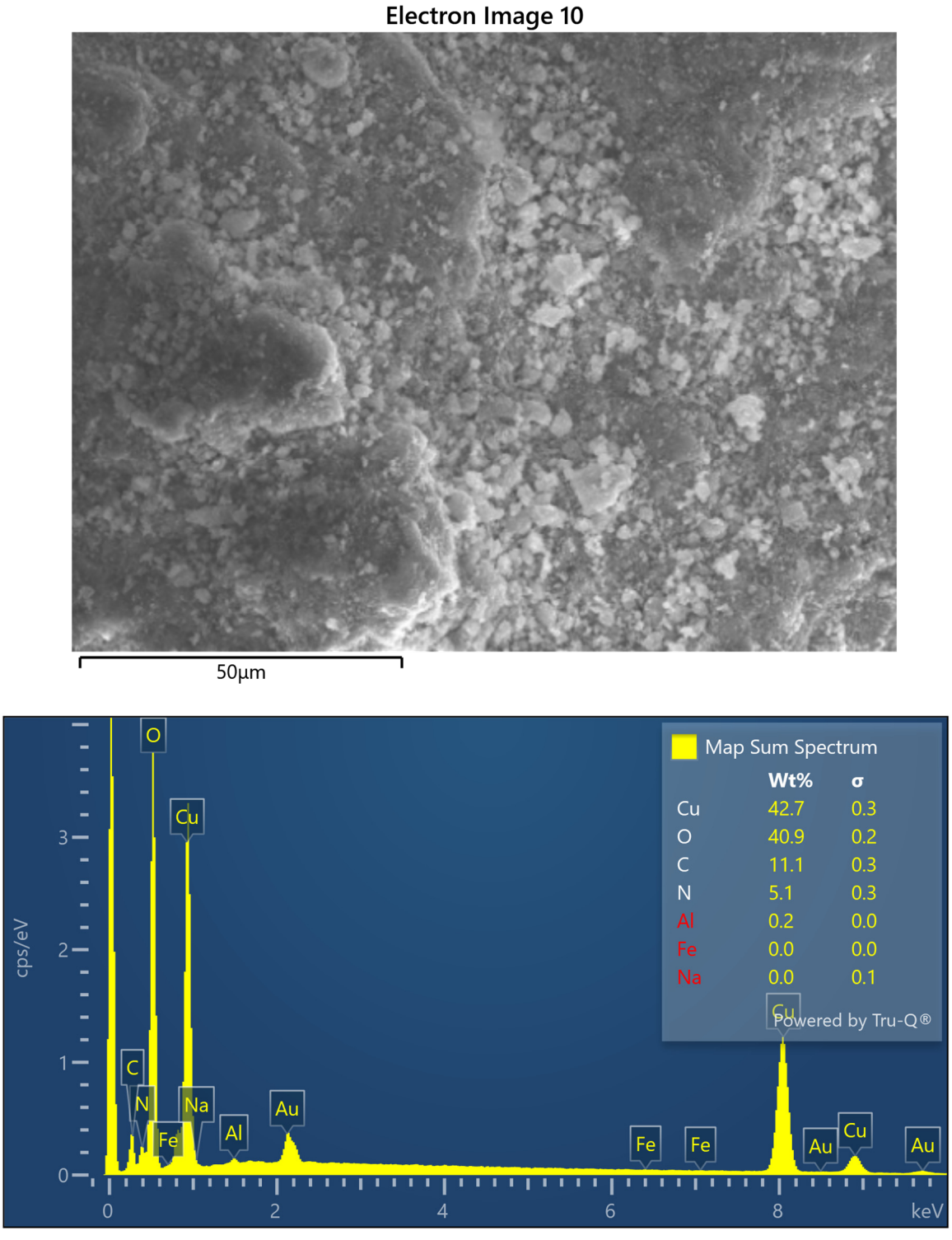

Figure S35: Surface morphology and elemental composition of Cu-TMC (spot 5).

Spot 6

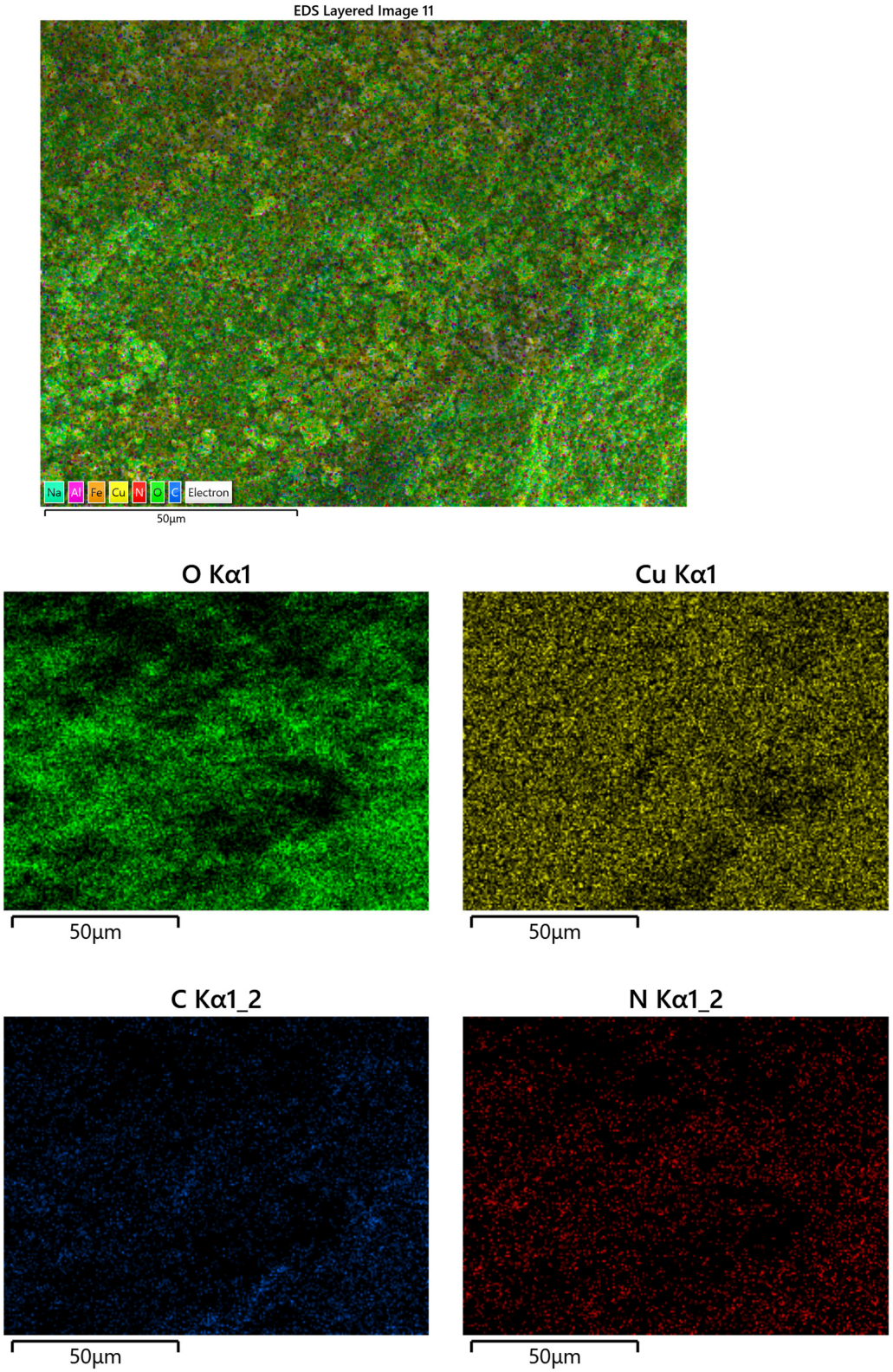

Figure S36: SEM-EDX mapping of Cu-TMC (spot 6).

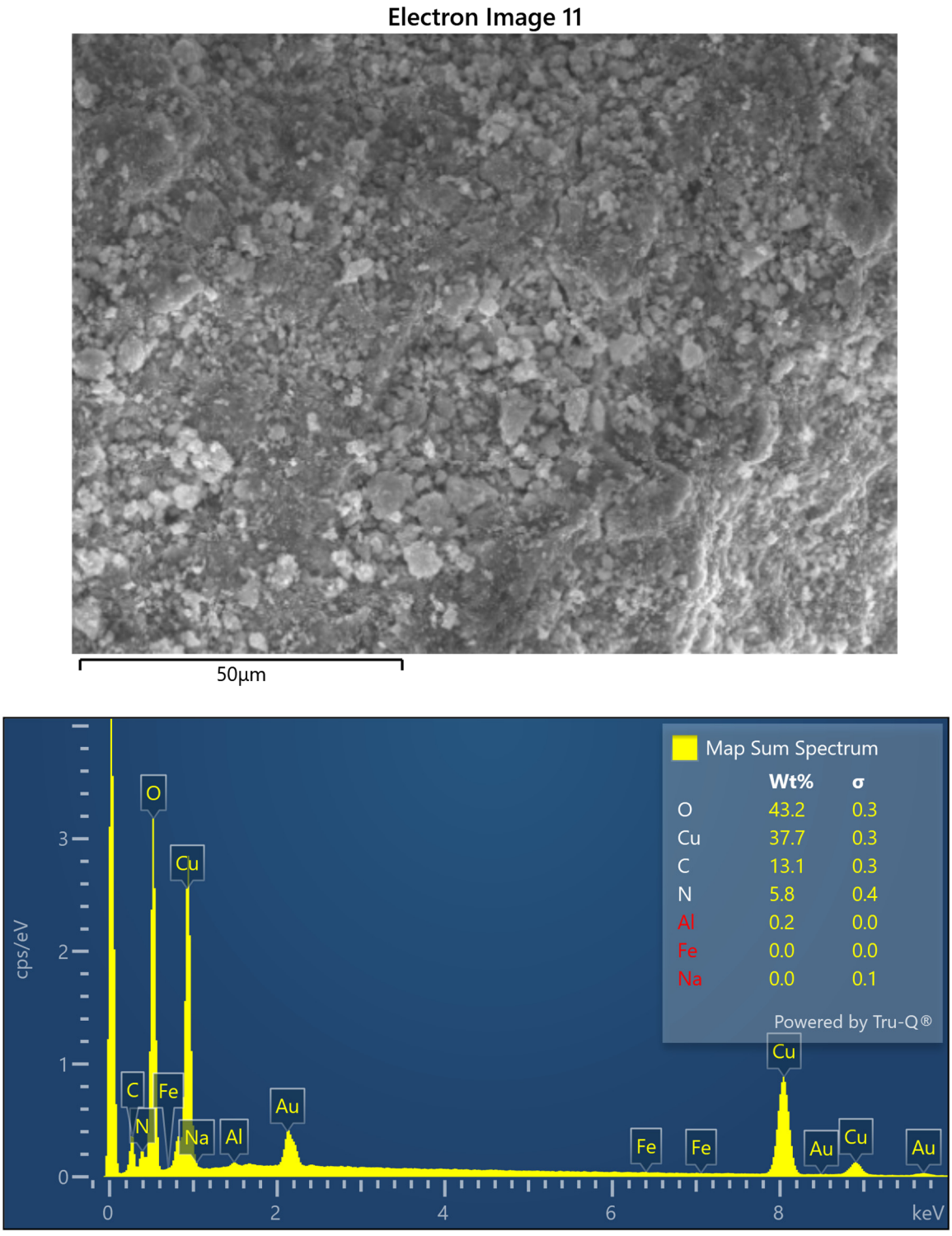

Figure S37: Surface morphology and elemental composition of Cu-TMC (spot 6).

Spot 7

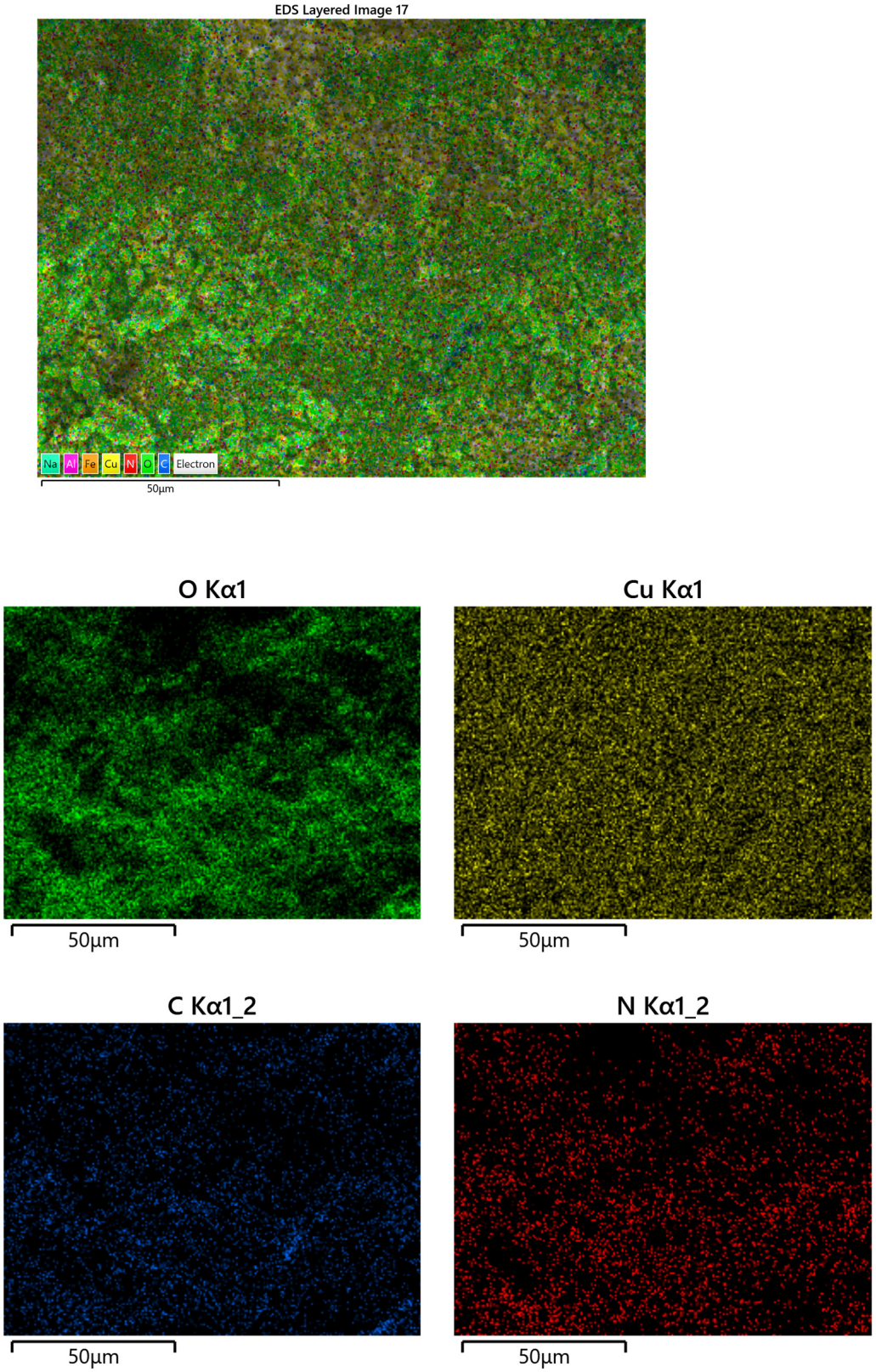

Figure S38: SEM-EDX mapping of Cu-TMC (spot 7).

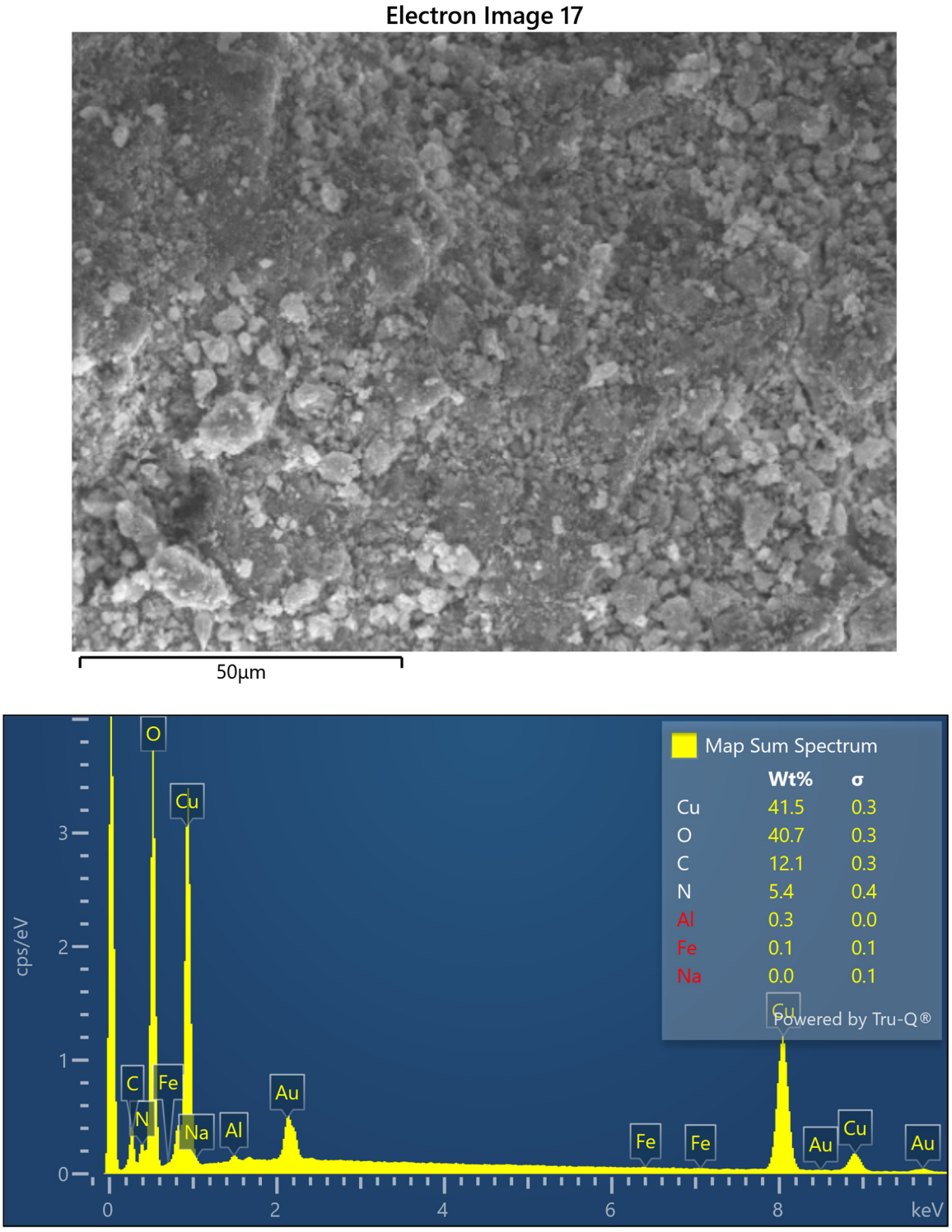

Figure S39: Surface morphology and elemental composition of Cu-TMC (spot 7).

Fe-TMC
Spot 1

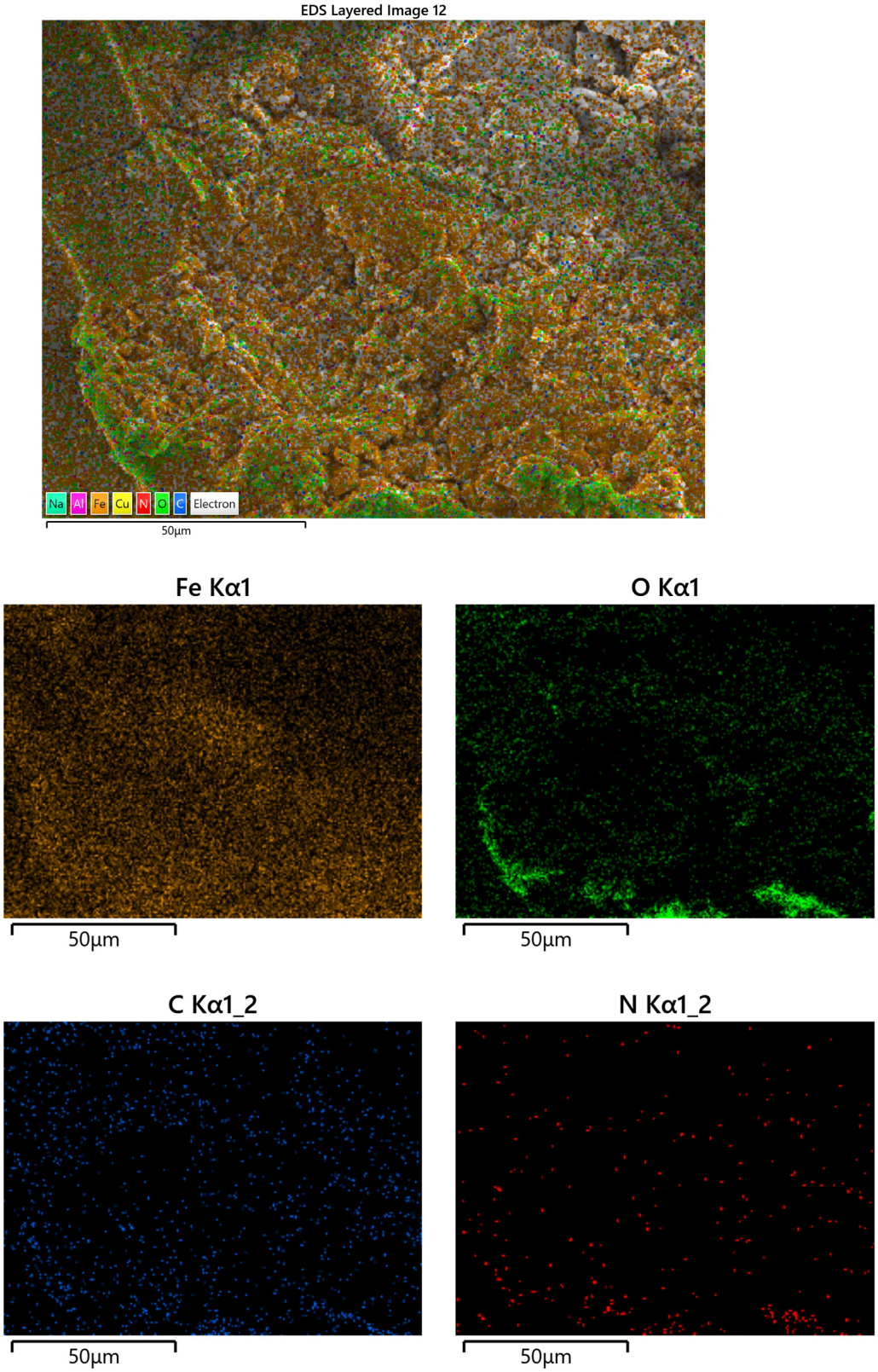

Figure S40: SEM-EDX mapping of Fe-TMC (spot 1).

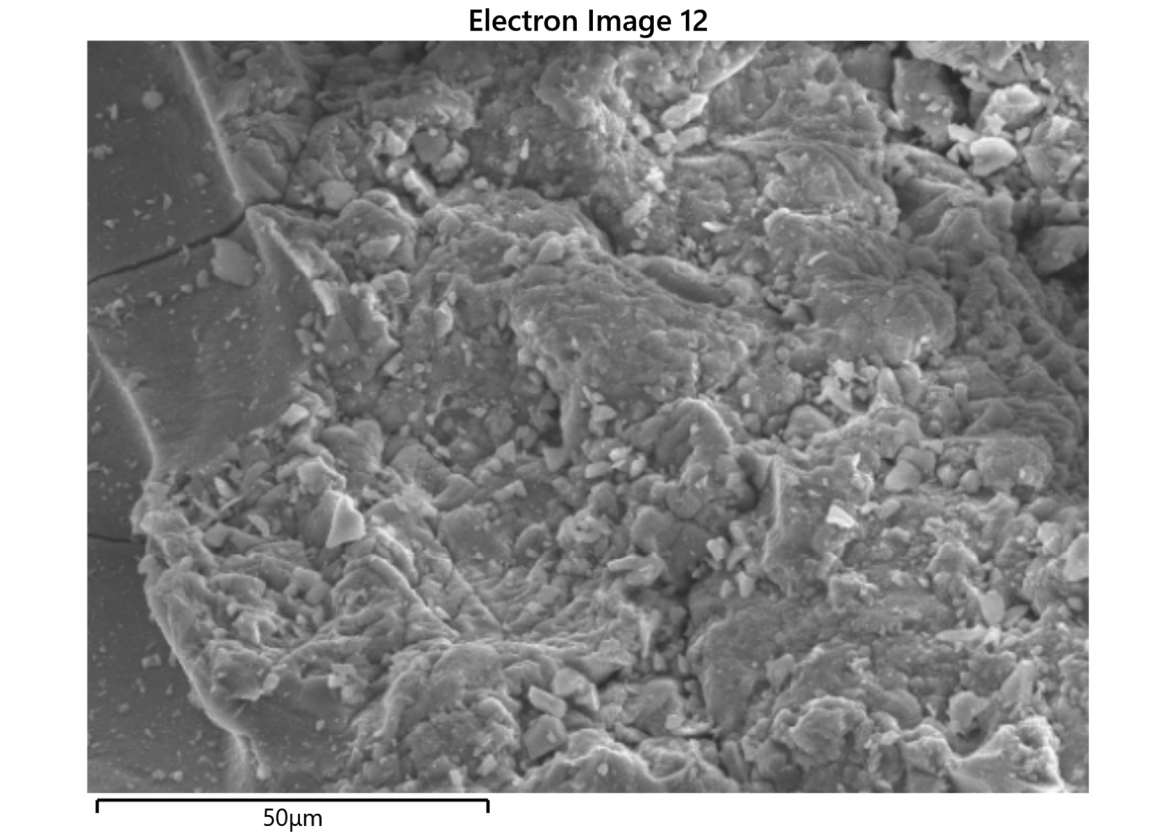

Figure S41:Surface morphology and elemental composition of Fe-TMC (spot 1).

Spot 2

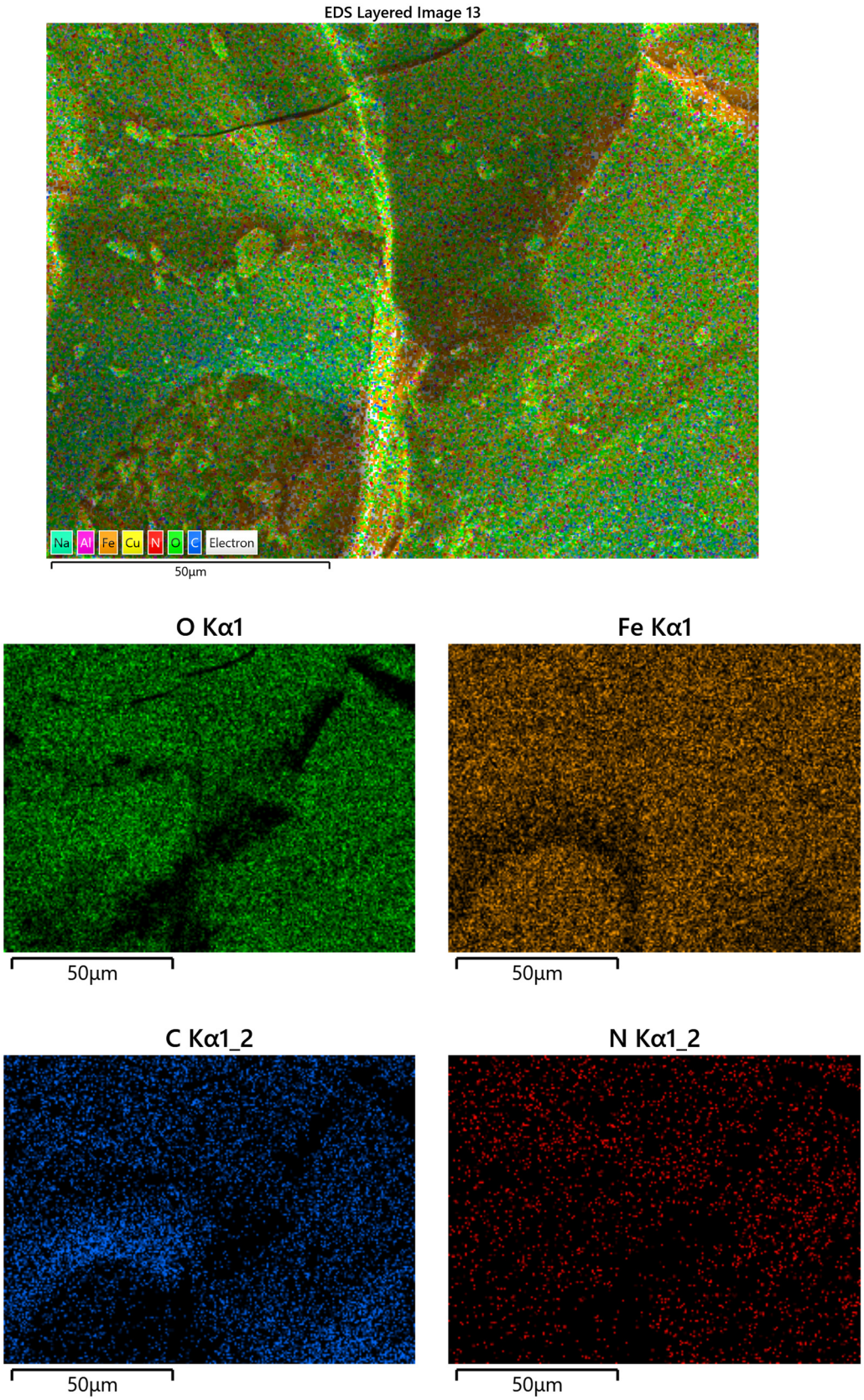

Figure S42: SEM-EDX mapping of Fe-TMC (spot 2).

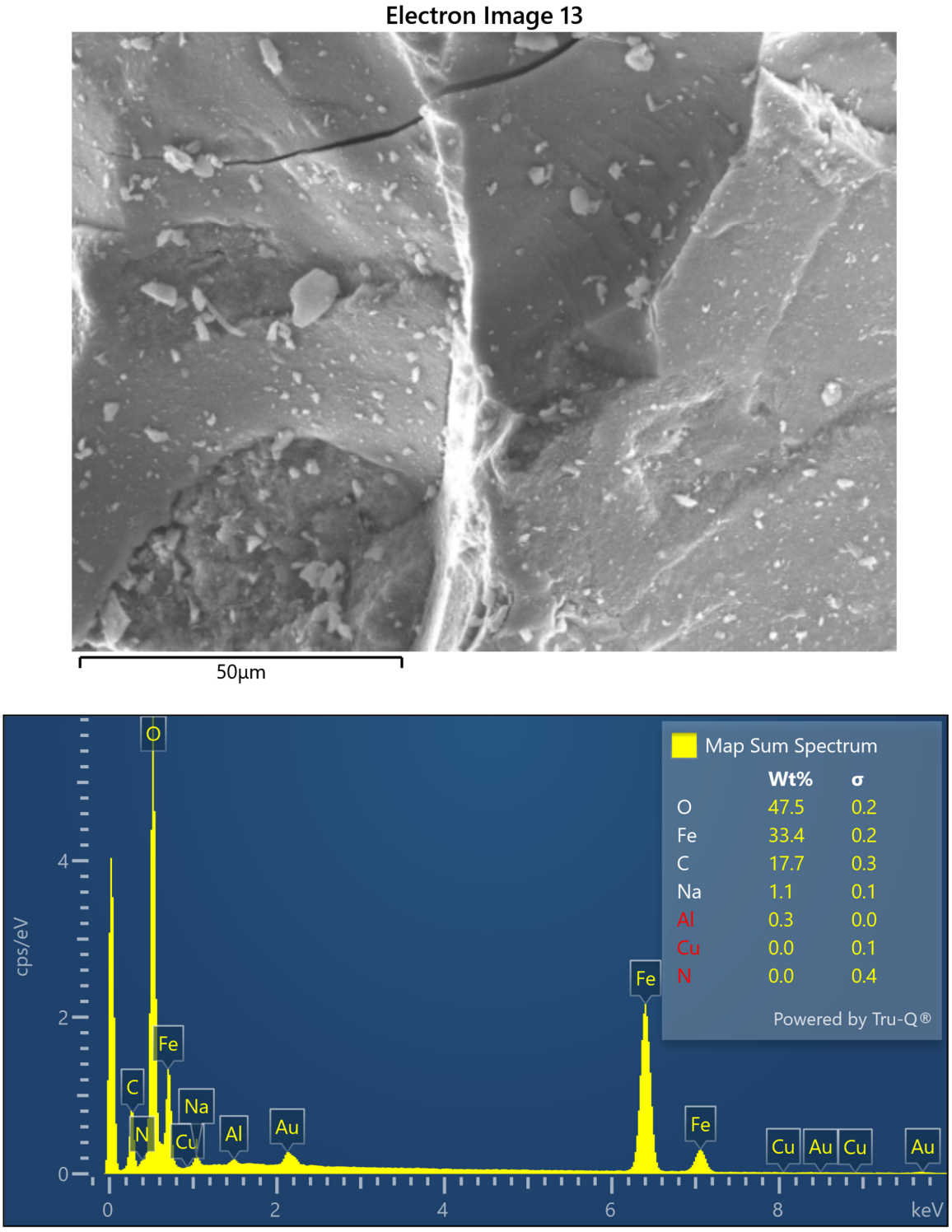

Figure S43: Surface morphology and elemental composition of Fe-TMC (spot 2).

Spot 3

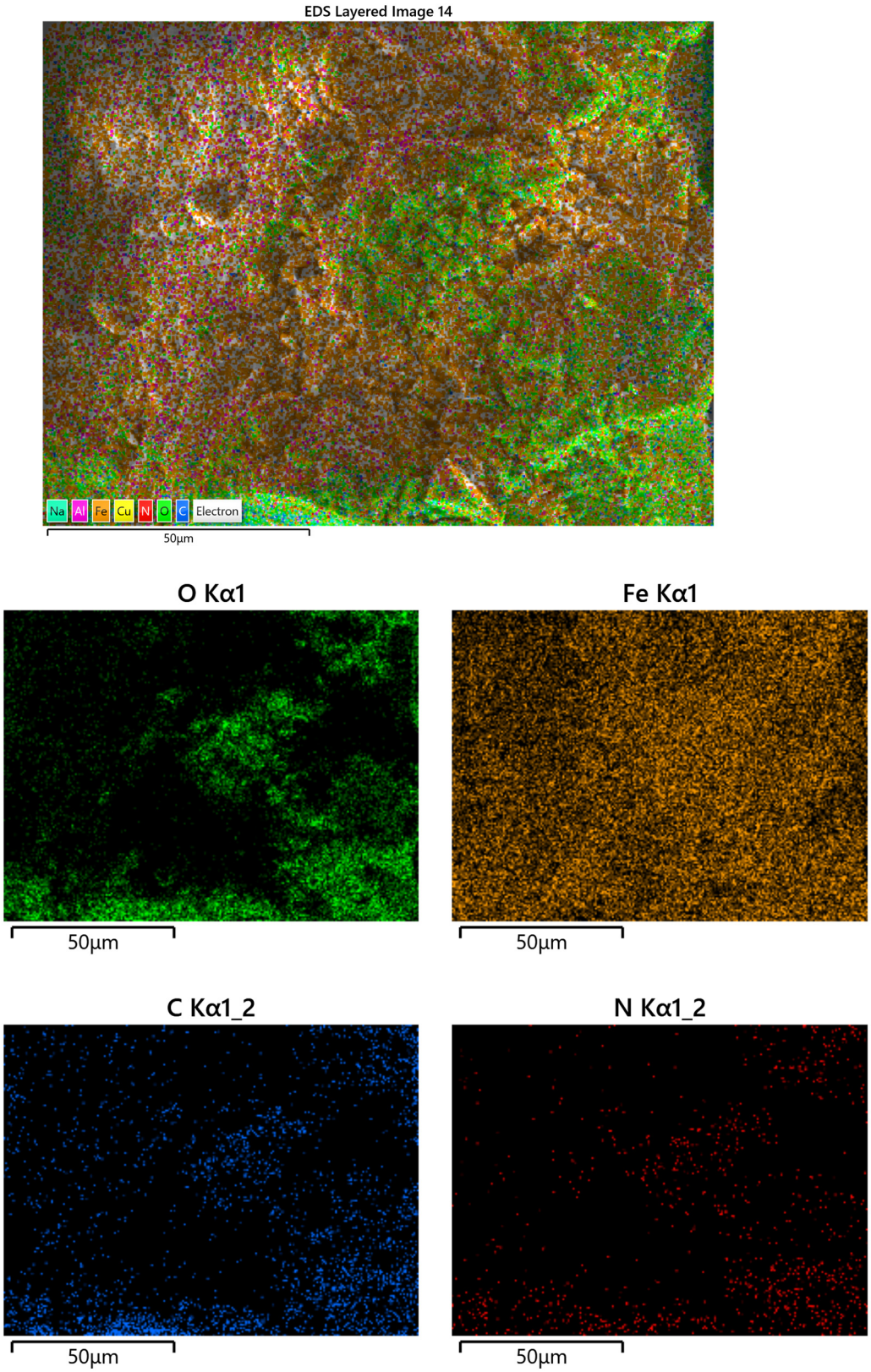

Figure S44: SEM-EDX mapping of Fe-TMC (spot 3).

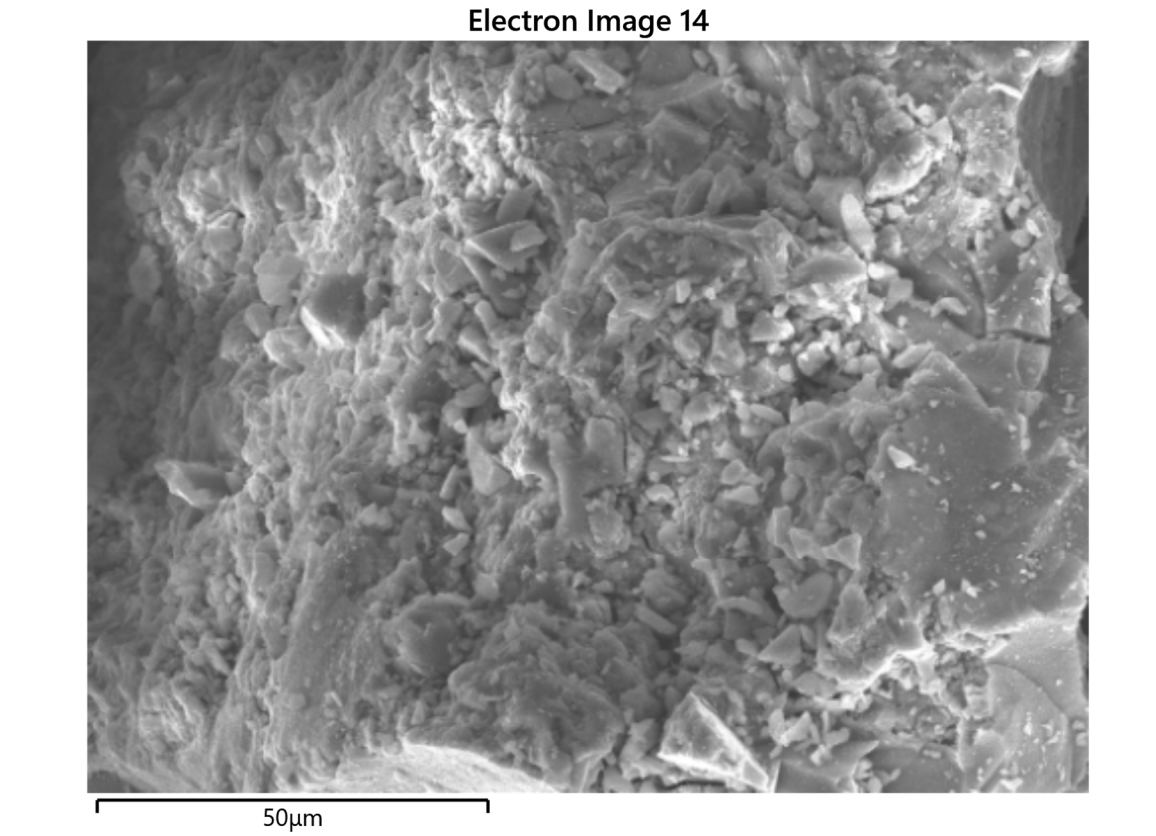

Figure S45: Surface morphology and elemental composition of Fe-TMC (spot 3).

Spot 4

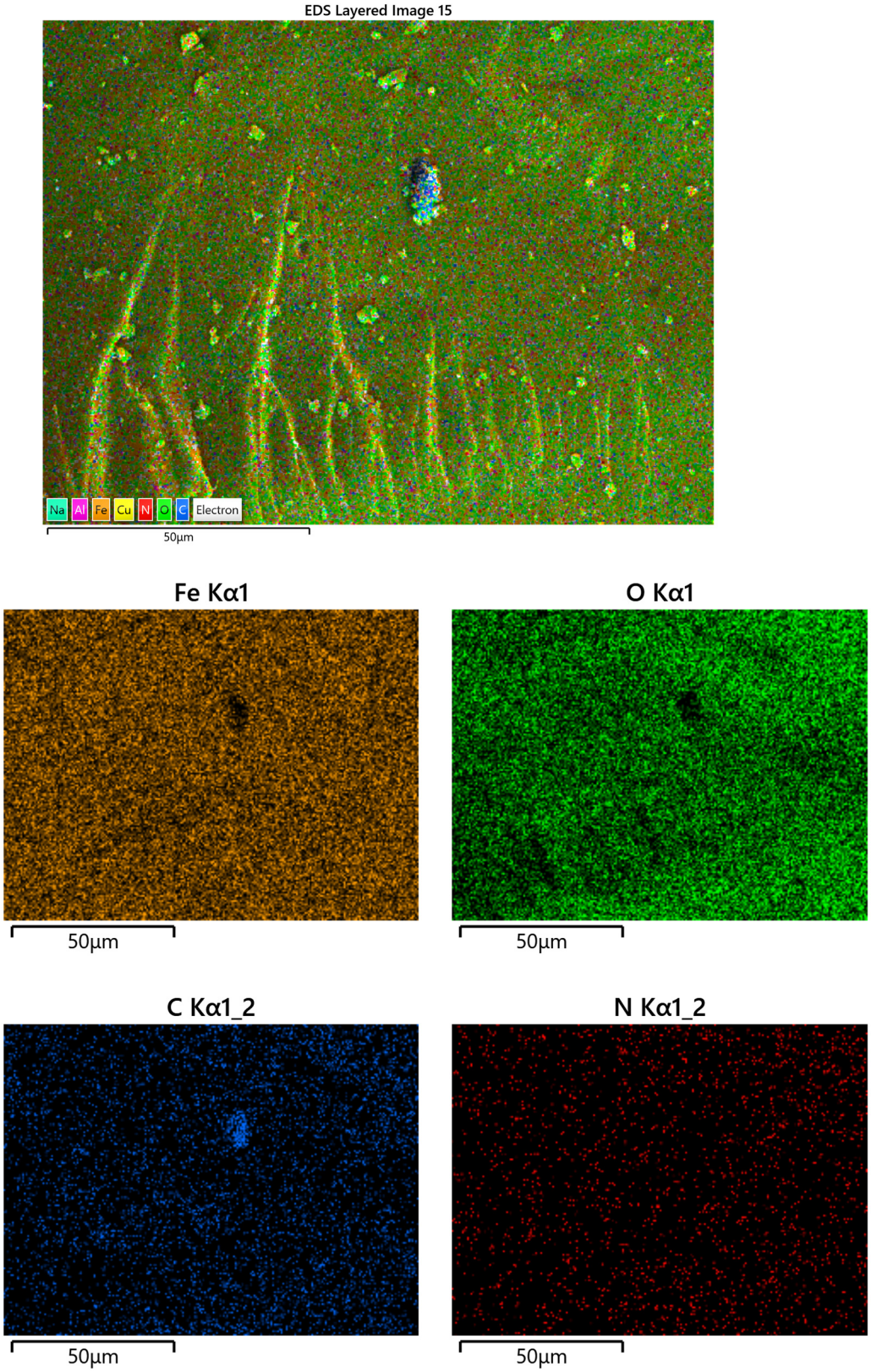

Figure S46: SEM-EDX mapping of Fe-TMC (spot 4).

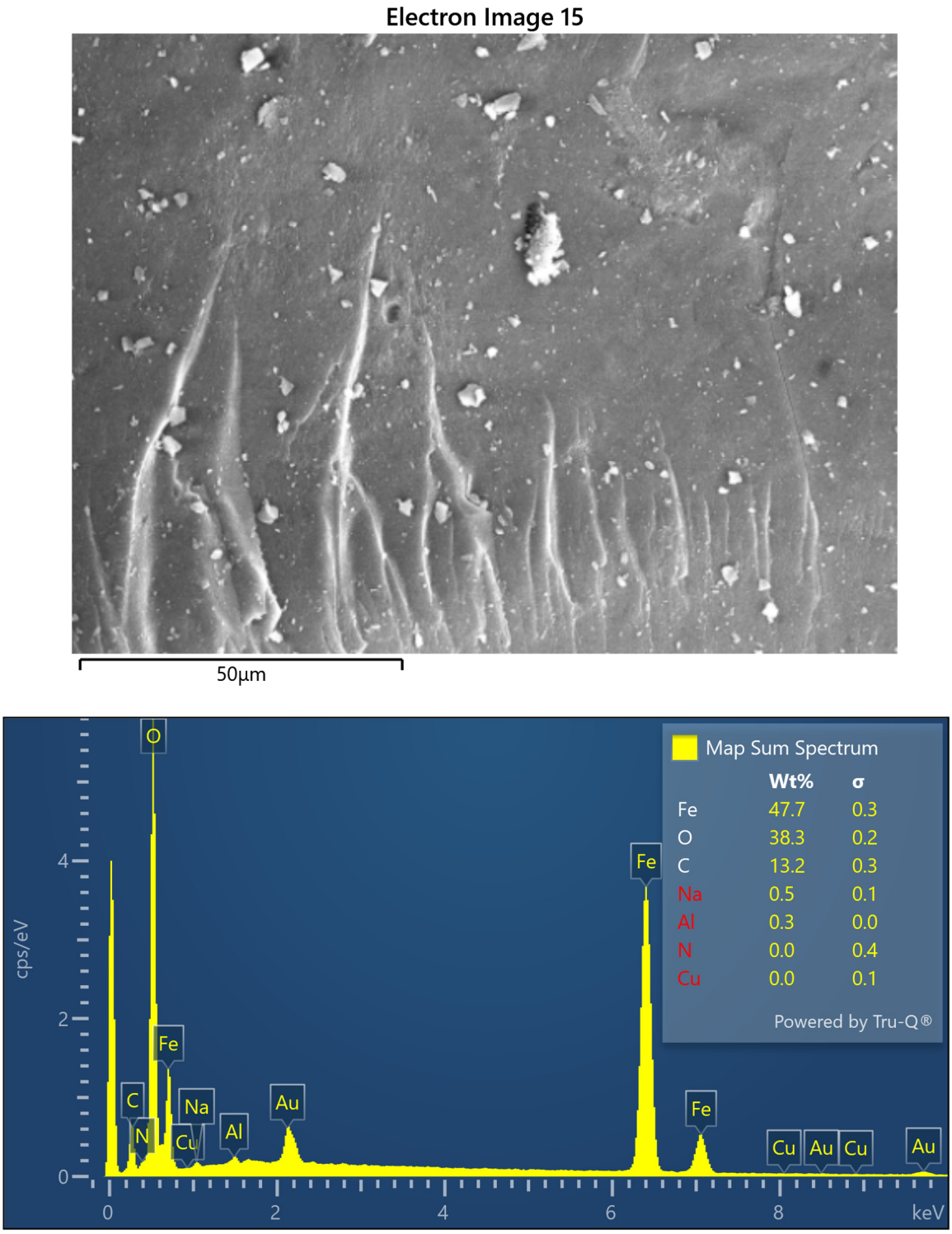

Figure S47: Surface morphology and elemental composition of Fe-TMC (spot 4).

Spot 5

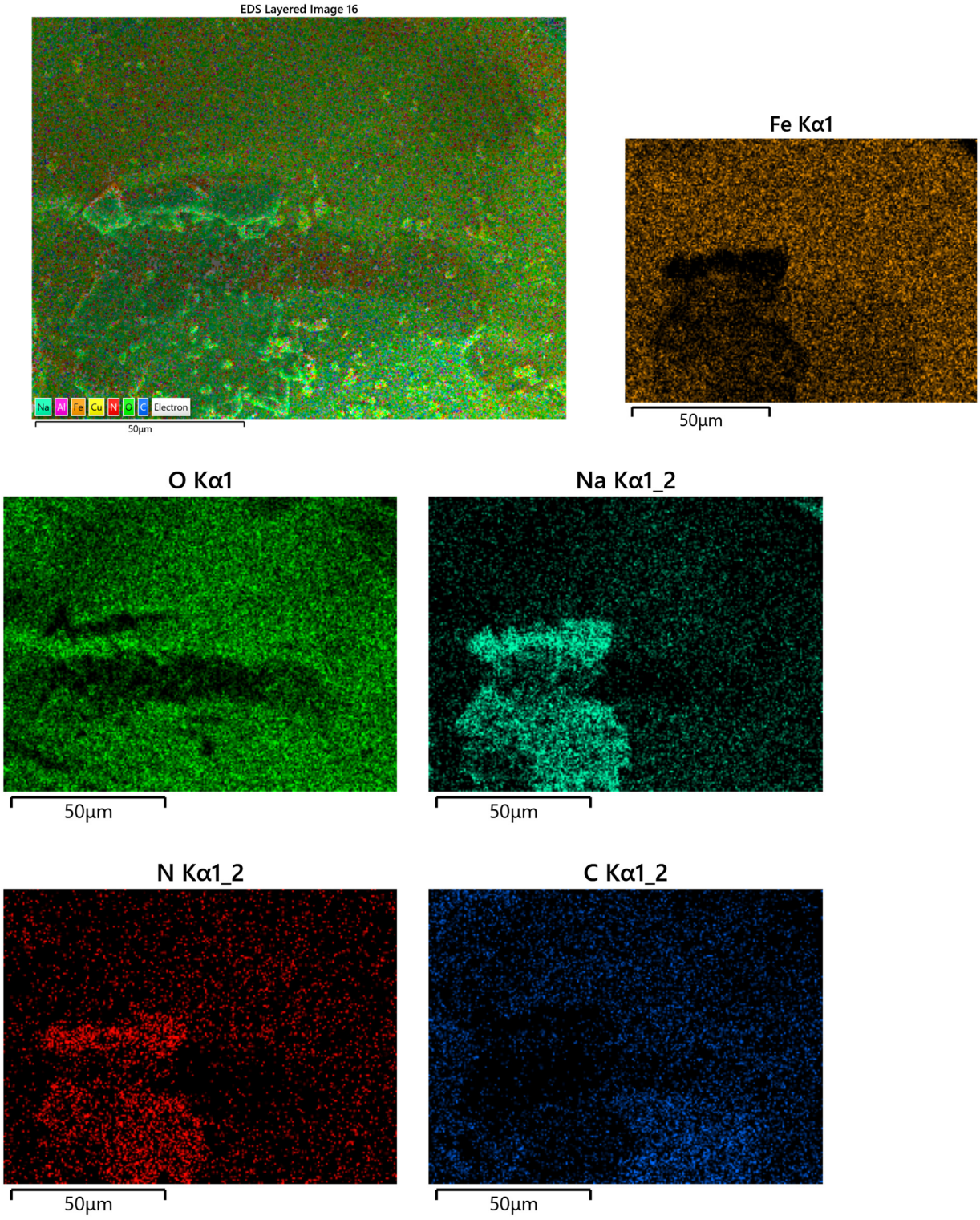

Figure S48: SEM-EDX mapping of Fe-TMC (spot 5).

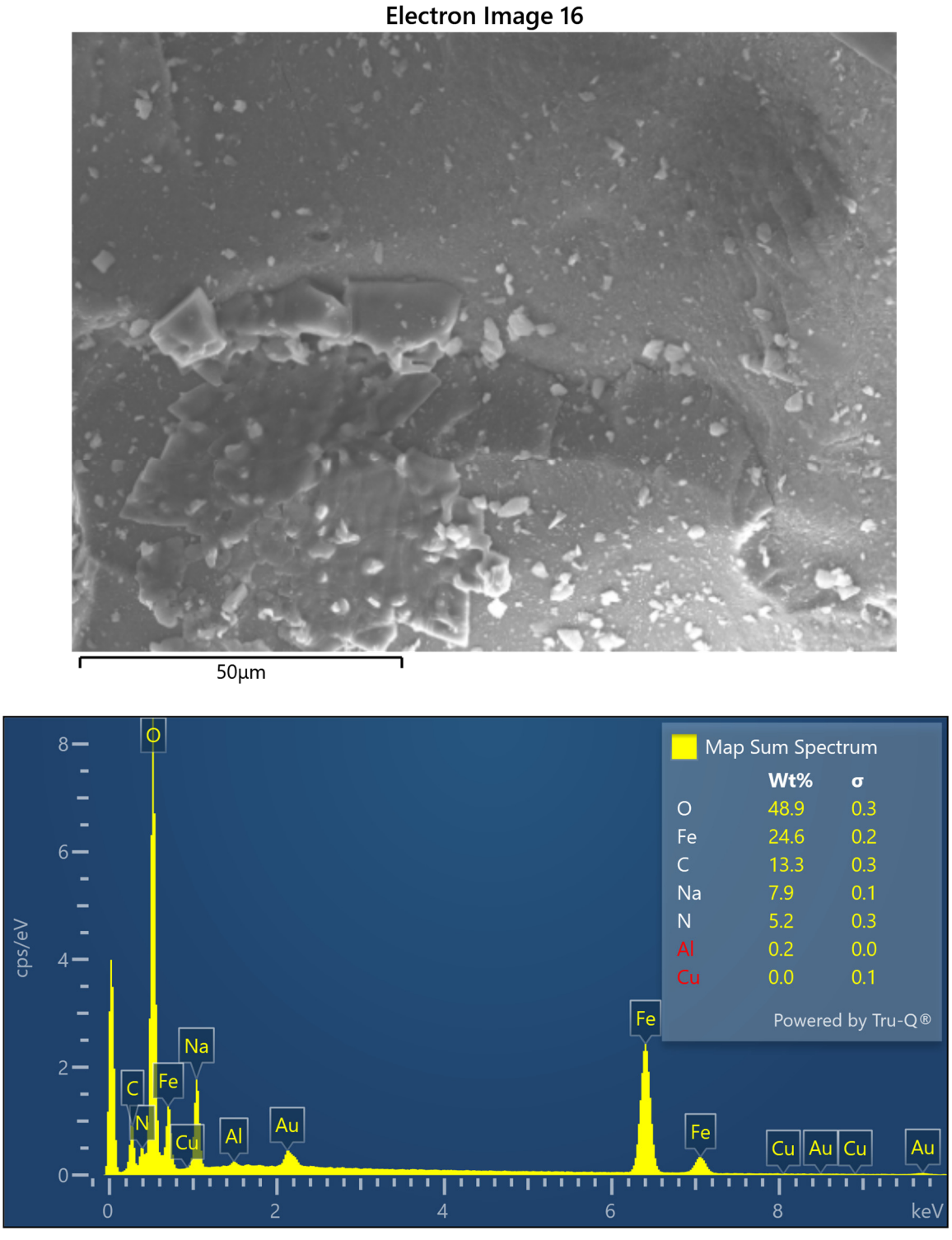

Figure S49: Surface morphology and elemental composition of Fe-TMC (spot 5).